



Hochschule  
Bonn-Rhein-Sieg  
University of Applied Sciences

**b-it** Bonn-Aachen  
International Center for  
Information Technology

R&D Project

# Dependency Detection for Sensor-based Fault Detection and Diagnosis

*Pooja Bhat*

Submitted to Hochschule Bonn-Rhein-Sieg,  
Department of Computer Science  
in partial fulfillment of the requirements for the degree  
of Master of Science in Autonomous Systems

Supervised by

Prof. Dr. Paul G. Ploeger  
M. Sc. Santosh Thoduka

January 2019



I, the undersigned below, declare that this work has not previously been submitted to this or any other university and that it is, unless otherwise stated, entirely my own work.

---

Date

---

Pooja Bhat



# Abstract

Design and implementation of Fault Detection and Diagnosis(FDD) methods is important when a system is provided with no immediate human intervention to prevent any catastrophic effect of the faults on the system environment or on the system itself. With the various approaches that have been proposed and developed for safety-critical systems, sensor-based fault detection and diagnosis(SFDD) has emerged and been widely adopted in the field of FDD for the autonomous systems, with the fact that any fault in sensor readings creates a wrong belief in a system, upon which it decides to act on the environment. In such SFDD methods, exploiting spatial and temporal dependencies among the sensor data streams is usually a primary requirement to assure faultless perceived values. Although correlation method appears as a straight forward solution for dependency detection, its inability to deal with certain corner cases often limit it in the application level. With an idea of implementing an alternate method to correlation, that provides for a more powerful tool for dependency detection, in this work, Granger causality, which captures Granger causal dependencies among the sensors has been implemented. The method is experimented on the Ropod Platform and the performance is analyzed. The results show that the method elegantly handles noise and lags in the signals and provides appreciable dependency detection, making it feasible for real-time applications.



## Acknowledgements

I thank Prof. Dr. Paul G. Plöger and M. Sc. Santosh Thoduka for providing me the opportunity to work on this Research and Development project. I have to specially thank M. Sc. Santosh Thoduka for his continuous guidance and valuable support throughout the project. I would like to thank Pranav Meherajan for his valuable suggestions to improve this work. Also, I thank Dharmin Bakaraniya for kindly helping me in understanding project related concepts. Finally, I extend my gratitude to my family and friends for their immense support and encouragement.



# Contents

<b>1</b>	<b>Introduction</b>	<b>1</b>
1.1	Motivation . . . . .	2
1.2	Challenges and Difficulties . . . . .	2
1.2.1	Recognizing and Choosing the Dependency Pattern . . . . .	2
1.2.2	Handling Miscellaneous Faults . . . . .	3
1.3	Problem Statement . . . . .	4
<b>2</b>	<b>State of the Art</b>	<b>7</b>
2.1	Sensor based Approaches for Fault Diagnosis . . . . .	7
2.2	Sensor Dependency Detection Methods . . . . .	9
2.2.1	Correlation-based Methods . . . . .	10
2.2.2	Copulas Theory . . . . .	11
2.2.3	Granger Causality Test . . . . .	12
2.3	Limitations of the Methods . . . . .	13
<b>3</b>	<b>Approach</b>	<b>15</b>
3.1	Granger Causality . . . . .	15
3.1.1	Definition . . . . .	15
3.1.2	Implication of Granger Causality . . . . .	16
3.2	Building Time Series Model for Granger Causality . . . . .	18
3.2.1	Time Series Analysis Models . . . . .	18
3.2.2	Bivariate VAR Model . . . . .	21
3.2.3	Granger Causality with Bivariate VAR Model . . . . .	22
3.3	Applying Granger Causality for Dependency Detection . . . . .	23

<b>4 Analysis of Behavior of Granger Causality</b>	<b>25</b>
4.1 Implementation Considerations . . . . .	25
4.2 Granger Causality on Sample Signals . . . . .	26
4.2.1 Linear Signals with Different Slopes . . . . .	26
4.2.2 Signals with Lag . . . . .	28
4.2.3 Signals with Noise . . . . .	32
4.3 Granger Causality on Sliding Window . . . . .	36
4.3.1 Effect of Window Size on Granger Causality . . . . .	36
4.3.2 Effect of noise on Granger Causality . . . . .	38
4.3.3 Effect of Changing Frequencies on Granger Causality . . . . .	39
4.4 Comparison of Granger Causality with other methods . . . . .	40
<b>5 Evaluation</b>	<b>41</b>
5.1 Hardware Setup . . . . .	41
5.1.1 Overview - The Ropod Platform . . . . .	41
5.1.2 Sensors in Ropod Smart Wheel . . . . .	42
5.2 Experimental Design . . . . .	43
5.2.1 Generating Different Motions with The Ropod Platform . . . . .	44
5.2.2 Injecting Faults into the System . . . . .	45
5.3 Evaluation Procedure . . . . .	46
<b>6 Experimental Results</b>	<b>49</b>
6.1 Evaluation in Torque Mode . . . . .	49
6.1.1 Defining Dependencies for Nominal Motions . . . . .	49
6.1.2 Dependency Detection with an Unplugged Wheel Encoder . . . . .	52
6.1.3 Dependency Detection with Disconnected Power Supply to a Motor	65
6.2 Evaluation in Velocity Mode . . . . .	69
6.2.1 Defining Nominal Dependencies . . . . .	70
6.2.2 Dependency Detection with an Unplugged Wheel Encoder . . . . .	70
<b>7 Conclusions</b>	<b>75</b>
7.1 Contributions . . . . .	76
7.2 Lessons learned . . . . .	76
7.3 Future work . . . . .	76

<b>Appendix A Nominal Signals from Ropod Platform</b>	<b>79</b>
<b>References</b>	<b>83</b>



# List of Figures

1.1	This figure shows four common types of sensor faults where unfilled circle represents normal behaviour and filled circle represents faulty behavior: (a) bias, (b) drifting, (c) complete failure/stuck, and (d) precision degradation [32]. . . . .	3
1.2	A sample structural model [6]. . . . .	4
2.1	Example of a sensor network with direct and indirect relationships modeled by cross-correlation analysis, where direct refers to the correlation relationship and indirect refers to relationship through a third element/entity [4]. . . . .	11
2.2	Example of a dependency graph modeled using Granger causality with six sensors with edges indicating existence of considerable dependencies [5]. . .	12
4.1	Linear signals with different slopes considered to analyze dependency. . . .	26
4.2	Results from all the three methods tested on the set of linear signals with different slopes. . . . .	27
4.3	Linear signals with different lags considered to analyze dependency. . . .	28
4.4	Results from all the three methods tested on the set of linear signals with same slope and different lags. . . . .	29
4.5	Sine waves considered to analyze dependency. . . . .	30
4.6	Results from all the three methods tested on the set of sinusoidal signals with different lags. . . . .	31
4.7	Noisy linear signals with different slopes considered to analyze dependency. .	32
4.8	Results from all the three methods tested on the set of noisy linear signals with different slopes. . . . .	33
4.9	Noisy sinusoidal signals with different amplitudes considered to analyze dependency. . . . .	34

4.10	Results from all the three methods tested on the set of noisy non-linear signals with different amplitudes. . . . .	35
4.11	Delay in response of Pearson coefficient and p-value due to window size. . . . .	37
4.12	Delay in response of Pearson coefficient and p-value due to window size. . . . .	39
4.13	Delay in response of Pearson coefficient and p-value due to window size. . . . .	40
5.1	The ropod platform with four smart wheels consisting of twin-wheels (figure 3.1b taken from preliminary results of the original project <a href="http://www.ropod.org/preliminary_results.html">http://www.ropod.org/preliminary_results.html</a> ) . . . . .	42
5.2	Schematic representation of smart wheel components (taken from design documents provided by Speciaal Machinefabriek Ketels VOF, Copyright of A. Ketels, 2017) . . . . .	43
5.3	Electronics cover of smart wheel removed (taken from the CAD drawings by Speciaal Machinefabriek Ketels VOF) . . . . .	45
5.4	Circuit board for ropod smart wheel . . . . .	46
6.1	Granger causal dependencies defined by p-values for nominal straight motion with lighter shades indicating dependencies. . . . .	50
6.2	Granger causal dependencies defined by p-values for nominal curved motions. . . . .	51
6.3	Granger causal dependencies defined by p-values for nominal on spot rotations. . . . .	51
6.4	p-values for straight motion with unplugged encoders. . . . .	52
6.5	Granger causal dependency diagrams for encoder 1 and 2 in nominal (left column) and faulty (right column) conditions in straight motion. . . . .	53
6.6	Change in p-value when fault is introduced by unplugging encoders. . . . .	54
6.7	p-values for curved left motion with unplugged encoders. . . . .	55
6.8	Granger causal dependency diagrams for encoder 1 and 2 in nominal (left column) and faulty (right column) conditions in curved left motion. . . . .	56
6.9	Change in p-value when fault is introduced by unplugging encoders. . . . .	57
6.10	p-values for curved right motion with unplugged encoders. . . . .	58
6.11	Granger causal dependency diagrams for encoder 1 and 2 in nominal (left column) and faulty (right column) conditions in curved right motion. . . . .	59
6.12	Change in p-value when fault is introduced by unplugging encoders. . . . .	60
6.13	p-values for on spot rotation in clockwise direction with unplugged encoder 1. . . . .	61

6.14	Granger causal dependency diagrams for encoder 1 and 2 in nominal (left column) and faulty (right column) conditions in on spot rotation in clockwise direction. . . . .	62
6.15	Change in p-values for on spot rotation in clockwise direction with unplugged encoder 1. . . . .	62
6.16	p-values for on spot rotation in anti-clockwise direction with unplugged encoder 1. . . . .	63
6.17	Granger causal dependency diagrams for encoder 1 and 2 in nominal (left column) and faulty (right column) conditions in on spot rotation in clockwise direction. . . . .	64
6.18	Change in p-values for on spot rotation in anti-clockwise direction with unplugged encoder 1. . . . .	65
6.19	p-values for straight motion with disconnected power supply to motor 2. .	66
6.20	p-values for curved motions when power supply to motor 2 is disconnected	67
6.21	p-values for on spot rotations when power supply to motor 2 is disconnected.	67
6.22	Change in p-values with disconnected power supply to motor 2 in straight motion. . . . .	68
6.23	Change in p-values with disconnected power supply to motor 2 in curved motions. . . . .	68
6.24	Change in p-values with disconnected power supply to motor 2 in on spot rotations. . . . .	69
6.25	Granger causal dependencies defined by p-values for nominal straight motion in velocity mode. . . . .	70
6.26	p-values for straight motion with unplugged encoders. . . . .	71
6.27	Granger causal dependency diagrams for encoder 1 and 2 in nominal (left column) and faulty (right column) conditions in straight motion in velocity mode. . . . .	72
6.28	p-values for straight motion with unplugged encoders. . . . .	73
A.1	Nominal sensed signals from straight motion in torque mode. . . . .	79
A.2	Nominal sensed signals from curved left motion in torque mode. . . . .	80
A.3	Nominal sensed signals from curved right in torque mode. . . . .	80

A.4	Nominal sensed signals from on spot rotation in clockwise direction in torque mode. . . . .	81
A.5	Nominal sensed signals from on spot rotation in anti-clockwise direction in torque mode. . . . .	81
A.6	Nominal sensed signals from straight motion in velocity mode. . . . .	82

## List of Tables

5.1 Table listing all the sensors available on a smart wheel with two wheels with a 3-phase BLDC motor each, along with corresponding sensed and derived variables with units. . . . .	44
--	----



## Introduction

As execution monitoring is a primary concern to assure safety and reliability of the systems, development of fault detection and diagnosis(FDD) methods is gaining more interest in the field of autonomous systems in the recent years. The faults associated with these complex systems highly vary and it is almost implausible to foresee every fault during system design stage. This makes the planning of FDD methods more complicated as they need to be capable to deal with various faults.

To provide quick detection, the faulty execution models can be used, but the unforeseen faults remain undetected [36]. Hence, to provide robust FDD, various generalized, on-line methods have been proposed. The Sensor-based Fault Detection and Diagnosis (SFDD) approach focused here, does not require any priori information, but it exploits the spatial and temporal dependencies among the sensor data streams to further use them for fault detection [27] [4] [15].

The approach aims to build a nominal model using sensor dependency information available in the system, to ensure normal execution. This can be explained with an example given in [27] i.e if a GPS sensor and an altimeter are present in the same system, they are redundant to each other for they both measure a common variable i.e altitude. This common variable measured by the redundant sensors are expected to be approximately equal in normal state. Any considerable violation of this dependency indicates a persisting fault in at least one element of the system. The natural dependencies existing in the system are hence continuously monitored by defining a formal relationship between the sensor components of system and checking for the existence of these pre-defined relationships to

ensure expected execution.

## 1.1 Motivation

Several complexities in robotic systems and high interaction with operating environment make them highly susceptible to faults. An autonomous system acts as an agent that maps between perception and actuation. It operates iteratively in a general pattern of sensing the environment through sensors, which creates a belief up on its surrounding, based on which it executes several commands with the help of various software and hardware components. For example, an ultrasonic sensor used for object detection, with each of its reading, induces a belief in the system up on distance of the object from itself. If this detected object is a target object and if the system is given a deviated value, the task to reach the target remains unaccomplished. Thus, sensor plays a vital role in the maintenance of a system's health. This undesired deviation from characteristic property of a sensor has to be validated, especially in harsh environments to prevent task failure.

Further, it uses the actuators to cause desired change in the environment. However, it is not always as desired, as the system is subjected to various noise and disturbances in real time and all the components involved in the process are vulnerable to faults. This requires the detection and diagnosis of the faults as soon as they occur to maintain right behaviour of the system. Thus, the intuition behind this approach is to prevent the propagation of fault from any sensor datastream/lower level to the execution level.

## 1.2 Challenges and Difficulties

While an intelligent control system has to provide self-supervisory operation to manage abnormal situations, there is a large domain of challenges that has to be encountered at every step, to enhance overall system dependability. Since, this work focuses on detecting the relationships among sensor data to analyse system health information, the associated challenges with it are discussed in this section.

### 1.2.1 Recognizing and Choosing the Dependency Pattern

Exploitation of various relationships among the sensor datastreams is a primary aspect of sensor-based fault detection and diagnosis (SFDD) methods. A complex system consists

of various sensor variables which exhibit spatial and temporal dependencies. This may occur due to several reasons that include:

- a. Measurement of the same parameter by the sensors.
- b. Actions of the system causing similar effect on the sensors.
- c. A sensor variable caused/affected by the other.

However, recognizing the relationship pattern that can be exploited is one of the challenges associated with sensor dependency detection.

### 1.2.2 Handling Miscellaneous Faults

The quality of sensors degrade as they age, especially when they are operated in harsh environment. Figure 1.1 illustrates common sensor faults, among which two in particular (stuck and drift) are hard to detect [27].

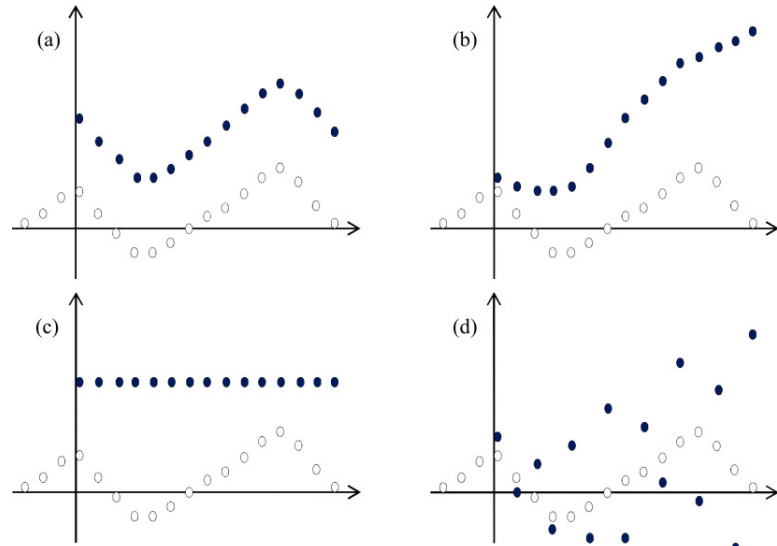


Figure 1.1: This figure shows four common types of sensor faults where unfilled circle represents normal behaviour and filled circle represents faulty behavior: (a) bias, (b) drifting, (c) complete failure/stuck, and (d) precision degradation [32].

When a sensor is stuck, it provides the same reading irrespective of the real state of the system. Drifting of the sensor causes reading to slowly increase or decrease from the

actual state. Since these type faults often fall in the correct range of the sensor, there is a high chance of them going undetected. Also, though these are generally categorised as abnormal behaviours, it is not impossible to find them in a healthy sensor that provides such reading as a mere response to current action of the system.

Hence, the methods designed for FDD is expected to be as robust and as general as possible to handle these faults and to provide dependable abnormal situation management.

### 1.3 Problem Statement

In [27], a structural model that infers the dependency of sensors on other components was proposed with a hypothesis that if a given component is faulty, then the fault is propagated to all of its dependent sensors and actuators. Figure 1.2 illustrates a sample structural model. In this work, a dependency detection method has to be implemented to

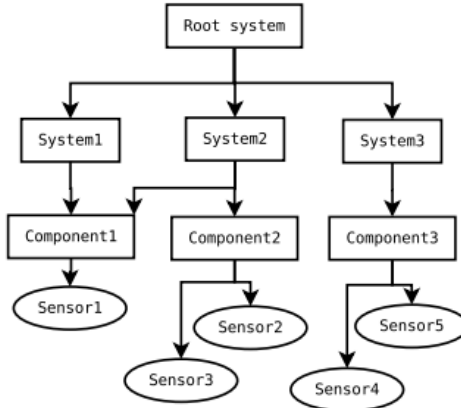


Figure 1.2: A sample structural model [6].

initiate bottom-up approach based on the hypothesis. To be specific, at every instant (in a window of predetermined size), when the sensors that are expected to hold a functional relationship, violate their dependency, the sensor that exhibits a suspicious pattern (such as drift/stuck) is considered to be faulty.

When a fault is found, this can be extended to higher levels such as when multiple sensors depending on the same component exhibit faulty behaviour, the hypothesis states that the component is faulty. The system elements are tested at each level until the faulty sensor/component/system is detected. Although correlation method that is originally

implemented in the work to detect sensor dependencies is an effective method, it doesn't perform well in the presence of noise and also fails in remote cases, for example, with a zero signal [6]. However, the dependency detection method plays a significant role to execute the approach in a way as simple as the concept. Thus, this work focuses on finding, implementing and experimenting a potential method that detects the relationships among sensor data streams and overcomes the shortcomings of the correlation method.

### **Objectives:**

- The selected dependency detection method should be light-weighted and provide fast analysis of relationships to provide on-line fault detection and diagnosis.
- The method should be capable of handling diverse signals and noise associated with them.
- The method should be able to exploit both spatial and temporal sensor dependencies.
- The model should be compatible with the structural model framework as far as possible.

---

### 1.3. Problem Statement

# 2

## State of the Art

In this chapter the approaches and methods proposed, evaluated and applied for the similar problems are discussed and the merits and demerits of the methods are analyzed. This provides a better understanding of the real-time system demands and capabilities of existing methods to set an idea of target performance of the method to be implemented in this work.

### 2.1 Sensor based Approaches for Fault Diagnosis

Identification of faults in sensors, referred to as sensor validation is a widely used approach in the field of fault detection and diagnosis [51]. The approach exploits the data from sensors and validates in two broad ways, either from a single sensor or from a set of sensor data streams. When single sensor data is considered to identify faults, the health information of the sensor is often provided by limit filtering or specifically, limit checking with a defined threshold [2]. The methods that exploit data from a set of sensors use the redundant information from the sensors, and are based on the principles of physical or analytical redundancy [4].

In a system, physical redundancy of sensors exists due to more than one sensor measuring the same parameter. In [16], drift of the sensor is corrected by detecting and accommodating intermittent and soft sensor faults with fuzzy principles using physical redundancy in the system. This involves inspection of differences existing among redundant sensors. Widely used analytical redundancy on the other hand assumes that a normal execution model is available and tend to use the functional relationships existing among

## 2.1. Sensor based Approaches for Fault Diagnosis

---

sensors. Here, the residual is obtained by comparing actual output with the nominal model. In [15] [3], authors define the non-redundant sensors with high correlation among them as quasiredundant sensors, and use data from multiple quasiredundant sensors to generate high confidence measure employing fuzzy logic rules and Parzen estimator respectively. Mainly used analytical redundancy based approaches also include Principal Component Analysis [11] [25].

One of the most popular analytical/model-based approaches is the Multiple Model Adaptive Estimation (MMAE) approach [21]. This approach is used in [44] for parallel prediction of outcome of several faults and to detect faults in wheeled mobile robots. For each type of fault, the system behavior is modeled and the models are embedded in several Kalman filters which are used as parallel estimators set to particular fault. The estimation of the sensor readings provided by the estimators are used to generate residuals from which faults are detected. This method applied to the case of mechanical failures were extended for 'hard' and 'soft' sensor failures in [45].

The MMAE approach falls in the class of non-interacting multiple models, as all the filters running simultaneously do not interact with each other. To overcome this problem and in particularly, to establish interaction among the models for the situations where sudden changes occur in the system modes frequently, in [20], Interacting Multiple Model (IMM) approach is proposed for a mobile robot, with 16 system modes consisting of one nominal and other hard failure modes. This work is extended in [21] to handle noise and scale failures using Variable Structure Interacting Multiple Model (VSIMM).

Although model-based techniques rely on a mathematical model describing the system to provide appreciable results and do not require redundancy in a system, the assumption of the existence of a perfect mathematical model of the system limits the performance [14], as the physical reality is beyond the reach of the model. Hence in [31], a model free, sensor based approach is introduced to detect anomalies in unmanned vehicles. The sensor readings form a cluster of observations and when every new observation/vector is provided by the sensor, it is compared with clusters using Mahalanobis distance. To reduce computational complexities, Dependency Detection (DD) is used to reduce cluster size [6].

In [26], the computational complexity of dependency detection is reduced using Pearson correlation coefficient and an on-line anomaly detection approach that relies on a sliding window is introduced. An on-line trainer method is to used find correlated sensors based

on the threshold given by correlation detector method where both the methods are fed inputs in a sliding window of size  $m$ . Then for every new vector (reading from the sensor), Mahalanobis distance is calculated with the correlated set of sensors and fault is declared if the threshold is crossed [6].

In [27], Sensor-based Fault Detection and Diagnosis used supervised structural model approach. This combined model-based approach with data driven approach to exploit advantages of both the methods. Based on the sensor inputs in sliding window fashion, faults were detected. This was further extended in [28], where a hybrid approach combining supervised and unsupervised learning was proposed.

In [4], the spatial and temporal relationships among sensors were exploited to provide cognitive fault diagnosis for distributed sensor network with an appropriate representation of functional graph and two-layer hierarchical architecture to diagnose faults. The layers include a processing layer that provides information based on change detection test (CDT), which in turn uses Hidden Markov Models that keeps track of the variations of relationships among sensors. The information is then integrated with graph representation to isolate the faults by cognition layer. The method was further extended to generate dependency graphs for fault diagnosis in [5].

Like some of the above mentioned approaches for sensor-based fault diagnosis, this work also aims to exploit information from multiple sensors for fault detection and diagnosis purpose. Since it is necessary to detect dependencies existing among sensors to use it for detection of faults, several promising methods that are used for dependency detection are explored in detail.

## 2.2 Sensor Dependency Detection Methods

Sensor dependency detection refers to identifying the existence of relationships among sensors that can justify the readings of a sensor based on the reading of the other, so when the reading is not justifiable with the reading of the related sensor, fault can be detected. Several methods are found in fault diagnosis literature to validate sensor readings to assure system reliability as mentioned earlier. In this section some potential methods used in previous work are discussed to understand their relevance and limitations.

### 2.2.1 Correlation-based Methods

Correlation being an intuitive way of detecting dependencies, is a popular dependency detection method. In a system, various sensors exhibit spatial and temporal correlation. While temporal correlation exists due to the effect of sensor readings observed at time  $t$  on the observation at time  $t + 1$ , spatial correlations occur due to identical readings of the sensors located at small distance from each other [34]. Here, the applications of correlation based methods in sensor dependency detection are discussed.

In [15] where quasiredundant sensors are used to increase confidence in the measurement, correlated and not necessarily redundant sensors are used. Virtual sensors are created in [35] to introduce redundancy in a ventilation unit. Since in all the components in the considered system work together, they share common principles and patterns. Hence, correlation used to exploit relations among measured quantities, that are not necessarily redundant. In [7], correlation among sensors are exploited to reduce false alarm rate in intensive care unit. In [27] and [6], Pearson correlation coefficient between sensor signals are used with an estimated threshold to further apply it for sensor-based fault detection and diagnosis.

In [33], a metric-correlation-based-distributed fault detection (MCDFD) is proposed for wireless sensor networks to detect faults when correlation between sensor nodes' system metrics that behaves normally in nominal state turns abnormal. Cumulative summation algorithm is used to keep track of these changes. This method aims to outperform highly expensive correlation inference models that sometimes may also fail to detect potentially faulty sensors that may not generate anomalous readings. In [39], semi-correlation was used to detect faults in vehicle control system.

As stated in [5], Bayesian frameworks also are used to model relationships among sensors [40]. In [18], Bayesian networks were used to provide spatial and temporal correlation among sensors for the enhancement of dependability in IoT applications. The effective representation and inference of dependencies provided by Bayesian Networks and its advantages over traditional correlation models was shown in [23]. In [56], Bayesian network was formalized using correlation in measurements at different sensors in medical body sensor networks.

In [4], dependency graph with nodes indicating sensors and edges indicating rela-

tionships defined by cross-correlation analysis was generated. The edge between couple of sensors existed when the maximum value given by cross-correlation was above defined threshold. The maximum value was obtained considering the peak value in cross correlation.

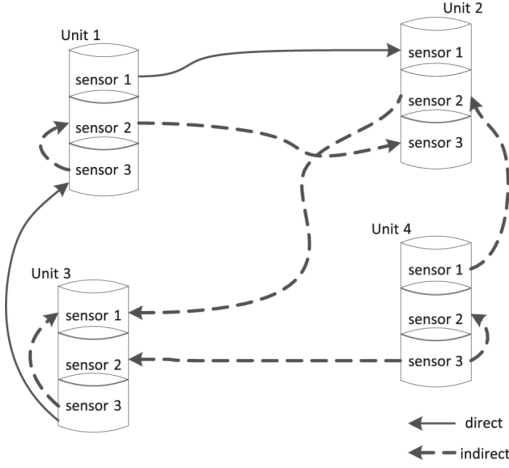


Figure 2.1: Example of a sensor network with direct and indirect relationships modeled by cross-correlation analysis, where direct refers to the correlation relationship and indirect refers to relationship through a third element/entity [4].

### 2.2.2 Copulas Theory

”A copula is a function which joins or couples a multivariate distribution function to its one-dimensional marginal distribution functions” [9] [41]. The dependence between several random models can be modeled using copula [22].

Based on the facts that correlation assumes observations to be conditionally independent and computation of correlation is expensive especially in the case of distributed detection system, copula approach is considered to model dependences between observations and is used to fuse correlated observations in [22]. Hence, the observations from three sensors fused to form a 3D model representing random variables in distribution detection system using copula is proposed in [22].

In [49] factors influencing the performance of the detection systems are stated to be affected by heterogeneity of the sensors existing due to difference in sensing ability,

quality control, duration of deployment etc and dependency in sensor observation due to measurement of same phenomena. The issues of heterogeneity of data and non-linear dependence existing among them are handled using copulas that describes the dependency information, in [49].

### 2.2.3 Granger Causality Test

Granger causality is a statistical hypothesis test based on the relationship that exists between two signals when one signal is able to predict the future values of other signal [17]. This statistical framework is used in [5] in exploiting temporal and spatial relationships among sensors to extend the dependency graph proposed in [4] and to establish cognitive fault detection and diagnosis.

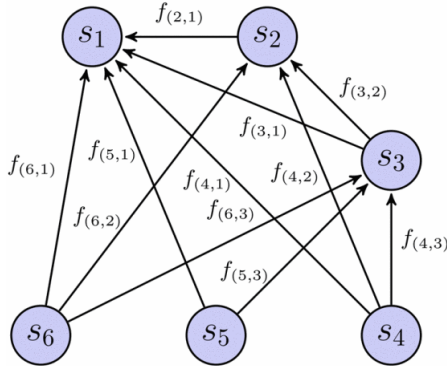


Figure 2.2: Example of a dependency graph modeled using Granger causality with six sensors with edges indicating existence of considerable dependencies [5].

[5] states that Granger causality is applied in various economic and medical applications, but, it has been applied for fault detection and diagnosis application for the first time in the literature. The cross-correlation analysis in the previous work is replaced by this method to establish functional relationships with multiple data stream and the issue of defining threshold does not exist in the method as it is easily tunable given a confidence level along with the dataset. This also provides a unique approach in terms of directionality as the dependencies between sensors are directed as shown in Fig.(2.2).

## 2.3 Limitations of the Methods

Some of the limitations of the above mentioned methods are listed here.

- Although from literature it is clear that correlation is widely used in sensor dependency detection, the method is shown to be highly sensitive to noise [6].
- In [5], the issue of sensitivity to noise is said to be existing also in cross-correlation along with lack of clear characterization of user-defined threshold, which is also true for correlation.
- The main drawback of Bayesian networks on the other hand, is the requirement of information or assumption on data generating process [5].
- In [8], it is said that traditional models have to be preferred over copulas if risk of the tails is not too high. Also, copulas is mathematically very intensive, computationally expensive and can slow down the model [12]. Since copulas requires full distribution of the data, it would also not fit for windowed data.

Granger causality appears to outperform correlation and cross-correlation from the results in [5]. Since the work here aims to fit in structural model proposed in [27], for on-line fault detection and diagnosis, Granger causality replacing a light weighted cross-correlation method in [5] seems suitable for the fast computation. Also, it promises to overcome issues in correlation like sensitivity to noise, making it an acceptable alternative for correlation in sensor-based fault detection and diagnosis. Thus, considering the drawbacks of the other methods and merits of Granger causality, Granger causality approach is selected in this work to detect functional dependencies in sensors.

### 2.3. Limitations of the Methods

# 3

## Approach

As described in section 1.2.1, sensor dependencies in a system occur due to various reasons. In this work, the dependency that exists due to the influence of one variable on the other variable is exploited. This is achieved by using causal dependencies, as proposed by Clive Granger(1969) in [17]. The concepts associated with the method is explained in detail in this chapter.

### 3.1 Granger Causality

#### 3.1.1 Definition

Granger causality is a statistical test to determine Granger causal relationship between time series. According to this, if the past values of time series Y can provide better prediction of another time series X than past values of X alone, then, Y causes X [52].

There are two principles associated with Granger causality [52]:

- The cause precedes its effect.
- The cause possesses additional information/unique information about the future values of the effect.

The definition of Granger causality can be explained using simple vector autoregression

model. Consider the following equations,

$$X(t) = a_0 + a_1x_{t-1} + a_2x_{t-2} \dots + a_px_{t-p} + \epsilon_{t1} \quad (3.1)$$

$$X(t) = a_0 + a_1x_{t-1} + a_2x_{t-2} \dots + a_px_{t-p} + b_1y_{t-1} + b_2y_{t-2} \dots + b_py_{t-p} + \epsilon_{t2} \quad (3.2)$$

The Eq.(3.1) and Eq.(3.2) form a model with two variables X and Y ( $n=2$ ). The model represents the evolution of  $n$  variables over time  $t$  ( $t = 1, 2, \dots, T$ ).  $a_0$  is a vector of intercepts,  $t - p$  refers to  $p$ th lag of the variable,  $a_i$  and  $b_i$  ( $i = 1, 2, \dots, p$ ) are time-invariants and  $\epsilon_{ti}$  are the error terms with mean zero [55].

The Eq.(3.1) provides the evolution of variable X as a linear function of its own past values. In Eq.(3.2), X is function of its own past values and the past values of Y. Fitting these models help to predict the influence of Y on X. Granger causality provides a statistical hypothesis that can be tested using a model that helps analyzing the dependencies of the fed variables. The result from the model helps in accepting or rejecting the hypothesis. The method for Granger causality hypothesis test is explained in detail later in this chapter.

### 3.1.2 Implication of Granger Causality

In this section, the definition of Granger causality is closely analyzed and is compared with methods that it is closely related to. This gives a better idea of the principles of Granger causality and what they actually imply.

#### Granger causality Vs. Causality

Granger causality is widely used in various fields such as, in neuroscience [47], and in economics, to predict various factors using available data (e.g causality between stock prices and economic growth [13]). Although Granger causality is often shortened for causality, it is important to note that it does not imply causality in actual sense.

Causality refers to a existing cause-effect relationship between two variables/processes [53]. Although in Granger causality, the signal that Granger causes the other signal is expected to precede it, it doesn't mean one signal is the cause for the other.

The difference can be better explained considering the underlying principle of necessary causes in causality explained in [53]. If a necessary cause between two variables/processes

$x$  and  $y$  exists such that  $y$  is necessary for  $x$  to occur, then presence of  $x$  implies  $y$  has occurred before. However, presence of  $y$  doesn't necessarily imply occurrence of  $x$  in future. This condition is not crucial in Granger causality. The true cause-effect between two variables does not exist, but one signal that precedes the other can be used for better prediction of its future values.

Though it is obvious to expect Granger causality to satisfy real causalities in the system, it is important to state the difference to justify non-obvious causal cases. For the remainder of the report, the term "causes" is used in place of "Granger causes" for brevity, but that does not indicate actual causality.

### Granger causality Vs. Correlation

It is evident from the definition of Granger causality and correlation, that both do not imply very similar relationships. If two signals  $X$  and  $Y$  are identical, they tend to exhibit high correlation, whereas the ability of either of the signals to predict the future values of the other is weak.

Consider two time series  $X(t)$  and  $Y(t)$  with mean  $\mu_X$  and  $\mu_Y$  and variance  $\sigma_X^2$  and  $\sigma_Y^2$  respectively. Then covariance and correlation between the time series is given by [19],

$$\text{cov}(X(t), Y(t)) = E((X(t) - \mu_X)(Y(t) - \mu_Y)) \quad (3.3)$$

$$\text{corr}(X(t), Y(t)) = \frac{\text{cov}(X(t), Y(t))}{\sigma_X \sigma_Y} \quad (3.4)$$

Granger causality between the series is given by [19],

$$X(t) = \sum_{j=1}^p A_{11j} X(t-j) + \sum_{j=1}^p A_{12j} Y(t-j) + E_1(t) \quad (3.5)$$

$$Y(t) = \sum_{j=1}^p A_{21j} X(t-j) + \sum_{j=1}^p A_{22j} Y(t-j) + E_2(t) \quad (3.6)$$

where  $E_j(t)$  refers to prediction errors. If variance of  $E_1(t)$  decreases in presence of  $A_{12j}$ , the "Y Granger causes X". This also applies to  $E_2(t)$  [19].

With the common factor of lag-lead relationship, it is more intuitive to compare Granger causality with cross-correlation. Considering the principles of Granger causality stated in the definition of Granger causality, cross-correlation defines a lag-lead relationship determining the correlation between two-signals with non-zero lag, hence satisfying the first principle (one signal precedes the other). However, Granger causality does more than that. Granger causality expects the leading signal to predict the future values of the lagging signal, which cross-correlation does not satisfy. This makes Granger causality a stricter inference. This property also makes Granger causality asymmetrical unlike cross-correlation [46].

Another difference between cross-correlation and Granger causality at the application level is that, cross-correlation draws different relationships due to auto-correlation coefficients. In Granger causality, autocorrelation coefficients are factored out and only cross-correlation coefficients are retained. This is why it indicates whether one signal can predict the other [10].

## 3.2 Building Time Series Model for Granger Causality

Time series is series of data points in the order of time [54]. As this definition covers sensor data, that is collected in time order, the data can be modeled as time series. The time series analysis is hence used to detect dependencies among sensors [30] [5]. This section elaborates on modeling time series. First, available time series analysis models that can be applied for Granger causality are discussed. Further, the model that is used is explained and integrated with Granger causality.

### 3.2.1 Time Series Analysis Models

Time series analysis consists of various methods to analyze the time-series data and collect its various characteristics. The models in time series analysis are used to predict future values based on the available past values. They represent stochastic processes and have many forms [54].

In this section frequently used time series models used with Granger causality are briefly discussed.

### **Vector Autoregression (VAR) Model**

Vector autoregression model can be used to detect linear interdependencies among multi time series data [55]. The univariate VAR model of order  $p$  (VAR( $p$ )) model can be described by following equation :

$$x_t = \alpha_0 + \alpha_1 x_{t-1} + \alpha_2 x_{t-2} \dots + \alpha_p x_{t-p} + \epsilon_t \quad (3.7)$$

The equation is used to forecast future values of the time-series. This can be extended for multi-variable examples, using a equation per variable. The variable  $p$  represents the lag considered in the equation for prediction. An appropriate lag to be considered to provide adequate forecasting is hard to find. Akaike Information Criterion(AIC) or Schwarz Information Criterion are used estimate best lag for to obtain appropriate model for forecasting. At each instant of time  $t$  the prediction of considered variable depends on its own past values and past values of other variables.

The given model is estimated by least squares method (ordinary least squares or generalized least squares). The difference between predicted and observed values can be compared to accuracy of the fitted model.

### **Vector Error Correction Model (VECM)**

This is a model specifically used for co-integrated variables. Based on the illustration given in [38], this can be explained with the example of a dog and a person who is holding the cord tied to the dog are both on a random walk, however, they are connected by the leash that keeps them connected. Such random processes are said to be co-integrated. Hence, two integrated variables are said to be co-integrated if a common stochastic trend is shared by the variables such that a linear combination of these variables is stationary <sup>1</sup> [29].

If a time series integrated of order  $d$  i.e  $I(d)$ , then it means discrete white noise is obtained by differencing the time-series  $d$  times[42]. The VAR framework is embedded with co-integration concept,to obtain VECM model. For the Eq.(3.7), VECM is given by [29],

$$\Delta x_t = \Pi x_{t-1} + \Gamma_1 \Delta x_{t-1} + \dots + \Gamma_{p-1} \Delta x_{t-p+1} + \epsilon_t \quad (3.8)$$

---

<sup>1</sup>Stationarity is the property of the time series whose statistical properties (mean,variance) are constant over time [1].

### 3.2. Building Time Series Model for Granger Causality

---

where  $\Pi = -(I_k - \alpha_1 - \dots - \alpha_p)$  and  $\Gamma_i = -(\alpha_i + 1 + \dots + \alpha_p)$ ,  $i = 1, \dots, p-1$ , k being number of variables considered.

There often exist several linearly independent co-integrated time-series. These co-integration relationships can hence be enforced on VAR model by re-parameterizing it and forming VECM model.

#### Autoregressive Moving Average (ARMA) Model

The ARMA(p,q) model is the fusion of Autoregressive(AR(p)) and Moving Average(MA(q)) models. AR(p) model is the univariate version of VAR model (same as restricted model in VAR). Though both of these are complete models, they are not used individually in Granger causality.

ARMA(p,d,q) can difference the non-stationary data  $d$  times to make it stationary. AR(p) model takes its past values as inputs and MA(q) characterizes white noise. An ARMA(p,q) model for time series  $x_t$  is given by[42],

$$x_t = \alpha_0 + w_t + \alpha_1 x_{t-1} + \alpha_2 x_{t-2} + \dots + \alpha_p x_{t-p} + \beta_0 + \beta_1 w_{t-1} + \beta_2 w_{t-2} + \dots \beta_q w_{t-q} \quad (3.9)$$

where  $w_t$  is the white noise and  $p$  and  $q$  are the orders of AR and MA models respectively. To get the best model with appropriate lag, Akaike Information Criterion(AIC)/Bayesian Information Criterion(BIC)/Ljung-Box test is used [42].

We can write Eq. 3.9 for ARMA(p,q) with  $\theta$  and  $\phi$  as functions of backshift operator  $B$  [42],

$$\theta_p B x_t = \phi_q B w_t$$

which when applied to a time series element, gives its previous element (one lag) [43].

In this work, bivariate VAR(p) model is used for Granger causality. Ideally, it is reasonable to try relevant methods and select based on the prediction accuracy of the models. However, the concern here is not to forecast the signals but to test if there is causality between the signals. In other words, one signal is not expected to accurately predict the future values of the other signal, but answer the question whether it can predict. Also, as this work aims to build bivariate relationship and to compare it with correlation method, a bivariate VAR(p), which uses Ordinary Least Squares(OLS) to fit

the model makes a sensible choice as it appears faster than ARMA(p,q) that deals with more parameters and uses Maximum Likelihood function for estimation which can be comparatively slower. Hence, though ARMA(p,q) handles non-stationarity well, VAR(p) model is chosen over it.

### 3.2.2 Bivariate VAR Model

Consider two variables x and y for the VAR model of order 1 VAR(1), i.e lag upto 1 unit time, observed at time t. The equations for the signals are given by [24],

$$x_t = \alpha_0^x + \alpha_1^x x_{t-1} + \alpha_2^x y_{t-1} + \epsilon_t^x \quad (3.10)$$

$$y_t = \alpha_0^y + \alpha_1^y x_{t-1} + \alpha_2^y y_{t-1} + \epsilon_t^y \quad (3.11)$$

The equations can be represented in matrix notation as,

$$\begin{bmatrix} x_t \\ y_t \end{bmatrix} = \begin{bmatrix} \alpha_0^x \\ \alpha_0^y \end{bmatrix} + \begin{bmatrix} \alpha_1^x & \alpha_2^x \\ \alpha_1^y & \alpha_2^y \end{bmatrix} \begin{bmatrix} x_{t-1} \\ y_{t-1} \end{bmatrix} + \begin{bmatrix} \epsilon_t^x \\ \epsilon_t^y \end{bmatrix}$$

As given in [24] this can be simplified as,

$$y_t = \alpha_0 + \alpha_1 y_{t-1} + \epsilon_t \quad (3.12)$$

$$\text{where } y_t = \begin{bmatrix} x_t \\ y_t \end{bmatrix}, \alpha_0 = \begin{bmatrix} \alpha_0^x \\ \alpha_0^y \end{bmatrix}, \alpha_1 = \begin{bmatrix} \alpha_1^x & \alpha_2^x \\ \alpha_1^y & \alpha_2^y \end{bmatrix}, \epsilon_t = \begin{bmatrix} \epsilon_t^x \\ \epsilon_t^y \end{bmatrix}$$

$\alpha_1$  measures the dynamic dependencies in y. This can be given as follows [37]:

- If  $\alpha_2^x = 0, \alpha_1^y \neq 0$

There is a unidirectional relation from x to y (y dependent on x).

- If  $\alpha_2^x \neq 0, \alpha_1^y = 0$

There is a unidirectional relation from y to x (x dependent on y).

- If  $\alpha_2^x = 0, \alpha_1^y = 0$

x and y are coupled.

- If  $\alpha_2^x \neq 0, \alpha_1^y \neq 0$

There is feedback relationship between x and y (output of one contributing the other).

To estimate the VAR model to draw conclusion on dependency between x and y, models for Eq.(3.10) and Eq.(3.11) are fit by least squares method.

### 3.2.3 Granger Causality with Bivariate VAR Model

Granger causality can be implemented using time series analysis models such as ARMA, VAR. In this section, the definition of Granger Causality is explained mathematically using bivariate VAR(p) model [50]. The coefficients defined in  $\alpha_1$  are estimated by least squares method in VAR model. The estimation result is further used for hypothesis test defined for Granger causality.

Considering the signals X and Y, equations to assess dependency of X on Y, following equations are defined using VAR(p) model.

$$X(t) = a_0 + a_1 x_{t-1} + a_2 x_{t-2} \dots + a_p x_{t-p} \quad (3.13)$$

$$X(t) = a_0 + a_1 x_{t-1} + a_2 x_{t-2} \dots + a_p x_{t-p} + b_1 y_{t-1} + b_2 y_{t-2} \dots + b_p y_{t-p} \quad (3.14)$$

The Eq.(3.13) is a reduced model where X is dependent only on its past values and Eq.(3.14) is a full model where X depends on past values of Y in addition to its own past values. A statistical test (t-test/F-test) can be applied to test the following null and alternate hypotheses:

$$H_0 : b_i = 0 \text{ for } i \text{ in } [1, p] \quad (\text{null hypothesis})$$

$$H_1 : b_i \neq 0 \text{ for at least 1 of } i \text{ for } i \text{ in } [1, p] \quad (\text{alternate hypothesis})$$

The null hypothesis  $H_0$  is accepted when Eq.(3.14) does not provide better prediction than Eq.(3.13) for future values of X. If not, null hypothesis is rejected and alternate hypothesis  $H_1$  is accepted indicating Y Granger causes X.

To apply a statistical test, the dependent variable (X in this case), is regressed on its past values using least squares method. This is called restricted regression (applied on the

restricted model), and from this, restricted sum of squared residuals are obtained. Further, the regression is computed using the unrestricted model that includes both dependent and independent variable, to obtain unrestricted sum of squared residuals. These residuals of both the models are compared to obtain F-value. If F-value is better than expected F-critical, then the null hypothesis is rejected [13].

The F-value is given as,

$$F = \frac{\frac{SSR_r - SSR_u}{p}}{\frac{SSR_u}{T-2p-1}} \quad (3.15)$$

where  $SSR_r$  and  $SSR_u$  are the sum of squared errors from restricted and unrestricted model respectively and the number of observations along with the lagged value  $p$  form the degrees of freedom  $T$ .

From the Eq.(3.15), if the error from the unrestricted model is almost equal to the error from restricted model ( $SSR_u \approx SSR_r$ ), full model does not provide better prediction. Thus, the more the difference between  $SSR_r$  and  $SSR_u$ , the higher the value of F, indicating the error with full model is low, that in turn proves the prediction with full model is better, hence rejecting the null hypothesis.

It is important to note that Granger Causality is sensitive to the number of lags considered in regression. This number represents the lag between two time series. To determine the proper number of lags, Akaike and Schwarz Information Criteria are used [13].

A simple Granger causality test can be applied for only two variables, for a defined number of lags. But, in the cases where more than one variable can influence the prediction, a multivariate Granger causality is used, including more than just two variables [13]. In this work, bivariate Granger causality is used to determine Granger causal relationship between two signals at a time.

### 3.3 Applying Granger Causality for Dependency Detection

In this work, the functional dependencies among sensors in a system are modeled using Granger causality with bivariate VAR as explained in the previous section. The proposed method aims to exploit Granger causal relationships between two sensor data streams.

### 3.3. Applying Granger Causality for Dependency Detection

---

The dependency detection method using Granger causality can be summarized as follows:

- For each pair of sensors defined in the system, provide the  $p$ , the best order to be considered in VAR model, based on previously mentioned Akaike/Schwarz Information Criterion, and the threshold value.
- Define restricted and unrestricted model to assess Granger causality.
- Estimate the model with least squares method in the VAR model.
- Obtain the sum of squared residuals for restricted and unrestricted models from the fitted least squares method.
- Apply F-test to test the hypothesis. If the F-value satisfies the confidence, reject null hypothesis.

In this work, `statsmodels.tsa.stattools.grangercausalitytests` module [48] is used to implement the method. The method here slightly differs from the above mentioned steps. The function does not determine the best order  $p$ , instead it is defined by the user. However, the maximum lag that can be fed is approximately one third of the size of the data. The function computes four statistical tests, two tests based on F-distribution and other two Chi-square distribution. The results from all the tests are similar. For all the F-value obtained from the tests, the corresponding p-values(probability values) are also provided. F-value and p-values are inversely proportional.

The F-value and p-values are given for each lag upto order  $p$ . Hence, to obtain a single p-value, the least p-value that falls in the defined confidence interval is considered. Thus, given the sensor data streams, lag  $p$ , and confidence interval, Granger causal dependencies between the the sensors can be determined.

# 4

## Analysis of Behavior of Granger Causality

Although the relevance of Granger causality for dependency detection is theoretically justified in the previous chapters, it is important to test the method on various signals for practical considerations. Hence, to understand the behavior of Granger causality, it is tested on some simulated signals similar to those considered in [6]. To draw conclusion on working of the method, the results are compared with correlation and cross-correlation for the same signals. This chapter describes the implementation of the method in detail.

### 4.1 Implementation Considerations

In the sensor-based fault detection implemented in [6] [27], correlation was used to detect sensor dependencies. Particularly, Pearson correlation coefficient was used to detect the dependency patterns in a system. In [4], dependency between sensors were accepted when the peak of the cross-correlation was above user-defined threshold. This method was further extended in [5], by replacing cross-correlation with Granger causality.

As mentioned earlier, in this work, Granger causality is compared with both cross-correlation and correlation to assess merits and demerits of Granger causality on various simulated signals. To do so, the p-value for Granger causality, Pearson correlation coefficient for correlation and the peak value of cross-correlation are taken in to consideration.

The p-value of Granger causality varies between 0 to 1, where  $p\text{-value} \leq 0.05$  denotes high dependency between the signals and  $>0.05$  denotes less likelihood of dependency. Pearson correlation coefficient varies between -1 to 1 with -1 denoting negative correlation,

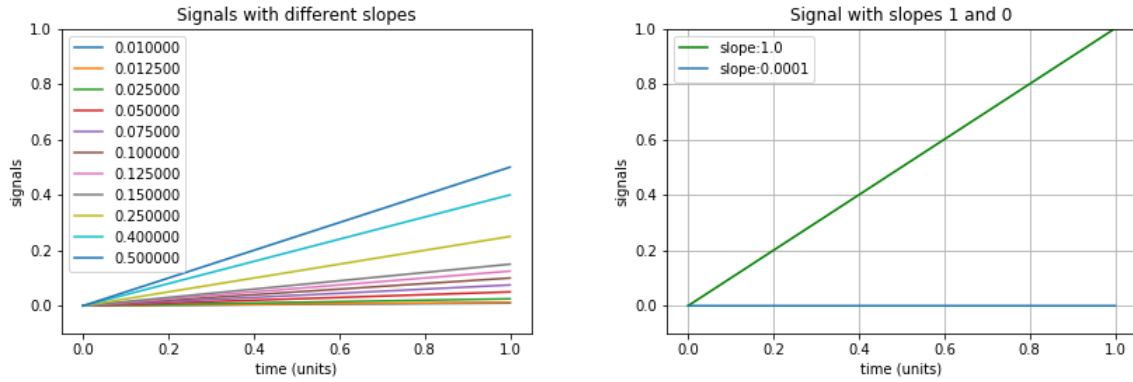
1 denoting positive correlation and 0 denoting no correlation. The convention also applies for cross-correlation.

## 4.2 Granger Causality on Sample Signals

In this section, the tests considering practical aspects are done similar to [6] where Pearson coefficient was used. Specifically, for similar set of signals, correlation with Pearson coefficient is repeated and in addition, Granger causality and cross-correlation methods are also tested and their results are analyzed. This helps in assessing the methods against practical aspects such as noise, lags in signals. The ability to handle such real-time issues proves the practicality of the method.

### 4.2.1 Linear Signals with Different Slopes

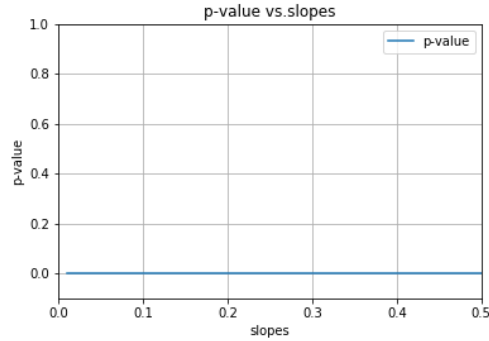
The methods are tested here on simple linear signals with various slopes. Linear signals with slopes ranging from 0.01 to 0.5 are generated and the dependency of each of these with linear signals with slope 1 and slope 0.001 are determined separately using each of the methods.



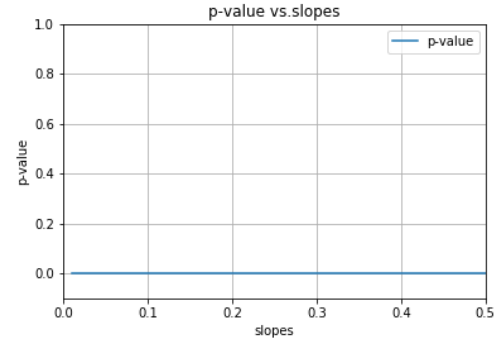
(a) Linear signals with increasing slopes.

(b) Linear signals to be dependent on.

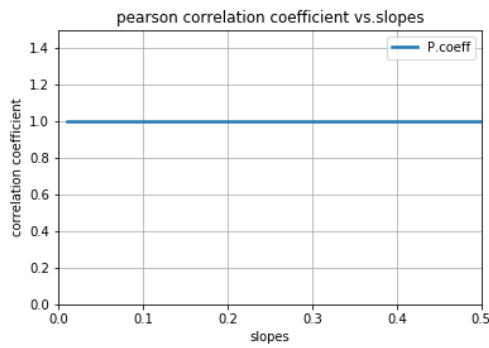
Figure 4.1: Linear signals with different slopes considered to analyze dependency.



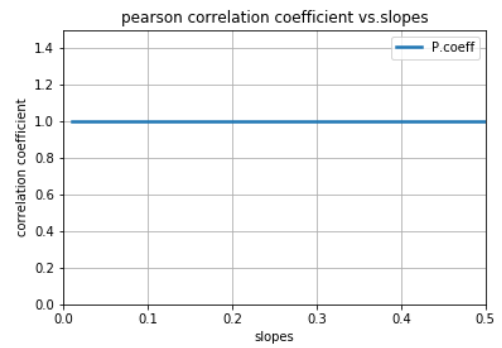
(a) p-value for the signal with slope 1.



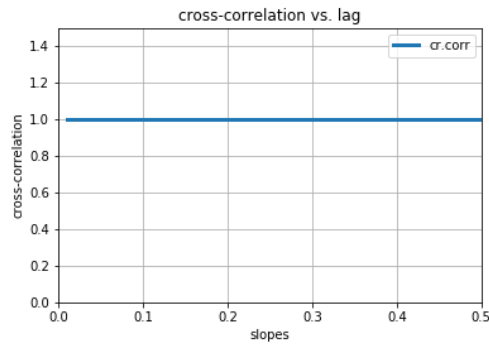
(b) p-value for the signal with slope 0.0001.



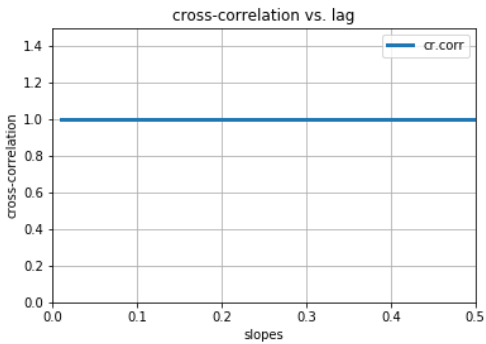
(c) Pearson coefficient for the signal with slope 1.



(d) Pearson coefficient for the signal with slope 0.0001.



(e) Cross-correlation for the signal with slope 1.



(f) Cross-correlation for the signal with slope 0.0001.

Figure 4.2: Results from all the three methods tested on the set of linear signals with different slopes.

As all the signals in Fig.(4.1a) increase with signals in Fig.(4.1b), they are expected to exhibit dependencies. As shown in the Fig.(4.2), all the methods indicate the dependencies between the signals with no regards to their slopes, even when compared to a signal with low slope 0.001. Also, results from all the methods are consistent and accurate. Thus, it can be concluded that slopes of the signals do not play any role in any of these methods.

### 4.2.2 Signals with Lag

As Granger causality claims to find dependencies on lag-lead relationship, it is important to assess the effect of lag in the signals on Granger causality. This section analyses all the three methods on signals with some time lag.

#### Linear Signals with Lag

In this section, the linear signals that increase together with some lag are used to test the effect of time lag of the signals on all the three methods.

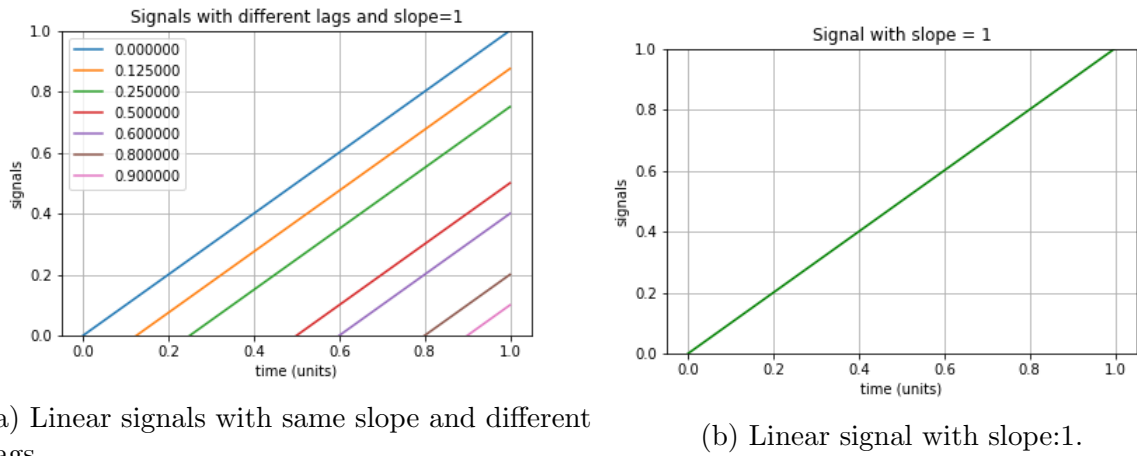


Figure 4.3: Linear signals with different lags considered to analyze dependency.

To test the influence of the lag in a signal with respect to the signal it is expected to show dependency with, some linear signals with same slope (i.e slope=1), with different lags ranging from 0 to 0.9 time units are generated. The dependency of each of these

signals with a linear signal increasing with slope 1, from 0 to 1 time units is assessed using all the methods. Though all the signals in Fig.(4.3a) do not start with the signal in Fig.(4.3b), their dependency is expected to be detected, as all of them increase together.

The results as shown in Fig.(4.4), detect the dependencies between the considered signals, irrespective of the time lag. Since, the results from all methods are consistent and accurate, it can be seen that time lags have no affect on the methods.

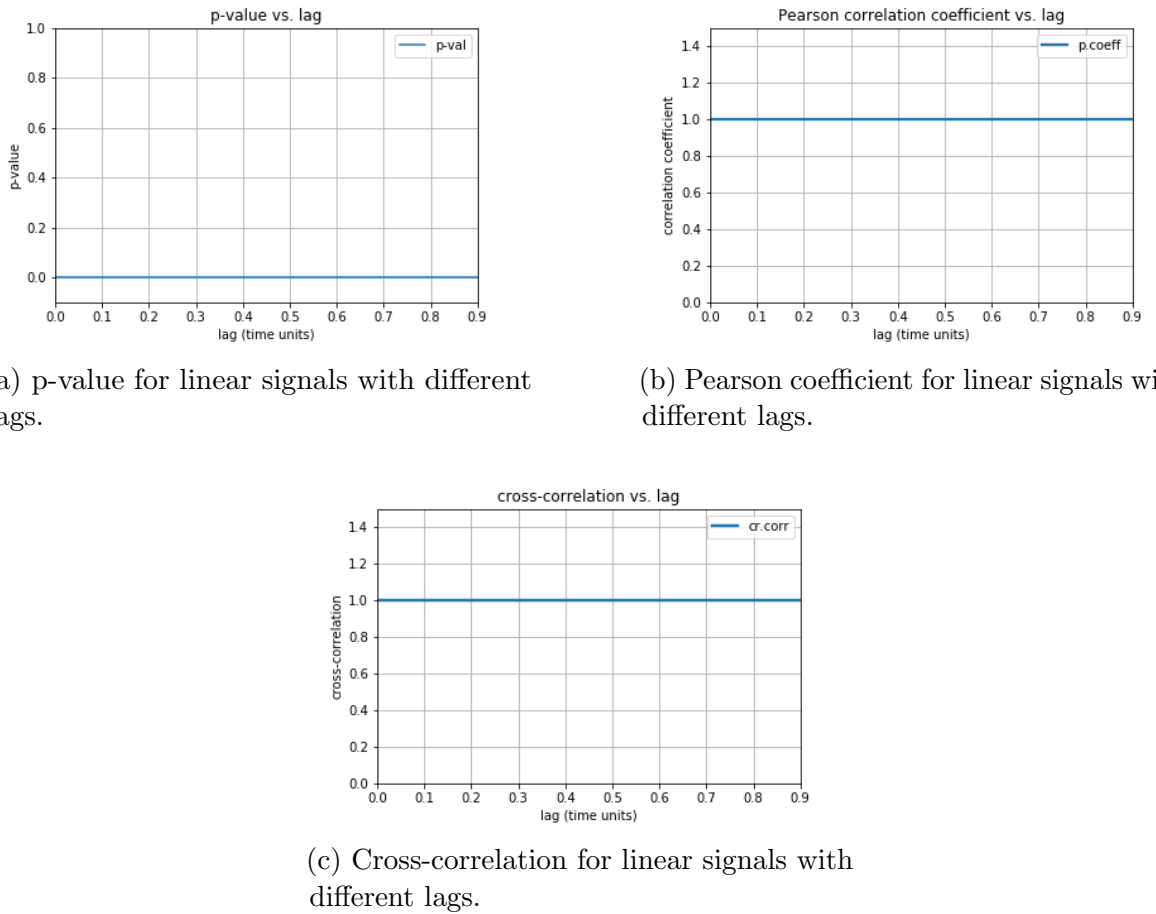


Figure 4.4: Results from all the three methods tested on the set of linear signals with same slope and different lags.

### Non-Linear Signals with Lag

In this case, the dependencies of sine waves with some lags shown in Fig.(4.5a) on the sine waves with different amplitudes (1 and 0.5) shown in Fig.(4.5b) are tested using all the three methods as in previous section. The three sine waves in Fig.(4.5a) start at different lags i.e  $\pi/4$ ,  $\pi/2$ ,  $3\pi/4$  (45, 90, 135 in degrees respectively) with respect to the sine waves in Fig.(4.5b).

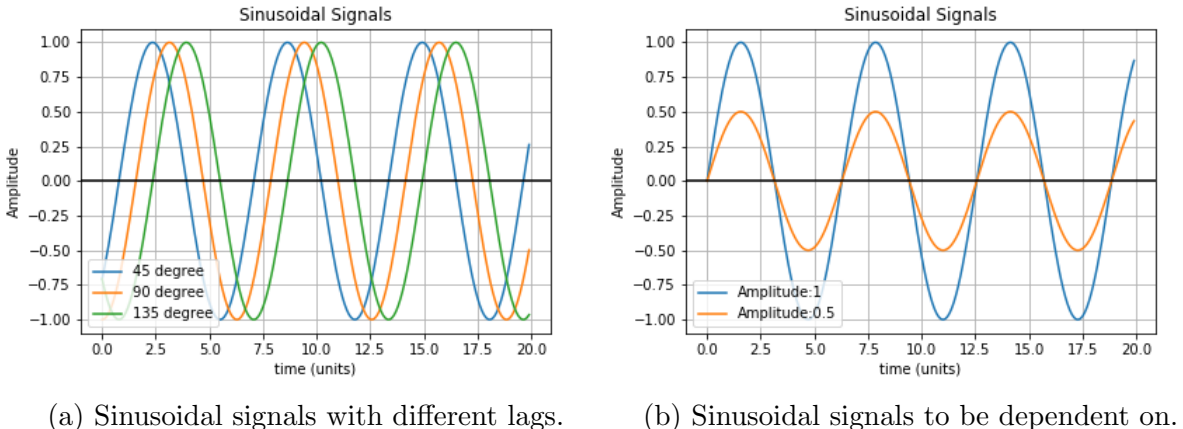
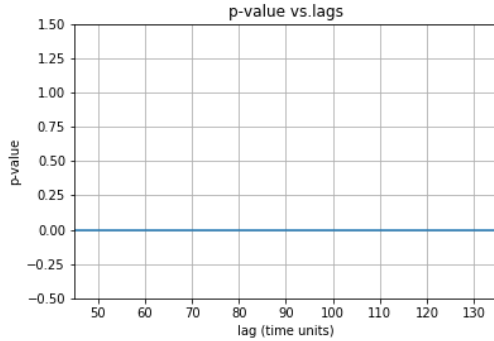


Figure 4.5: Sine waves considered to analyze dependency.

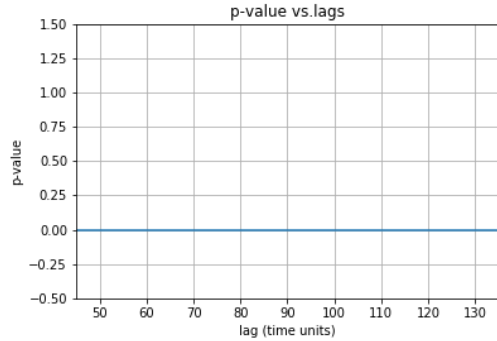
In the previous section, it was shown that lag in the linear signals did not affect the results of any of the considered methods. However, it is difficult to conclude that lags do not affect the results in any case from the results observed from the data that is continuously increasing. Lags in non-linear data can be more difficult to handle. For example, in the considered sine waves, with the increase in lag, crests and troughs partially overlap. This may confuse dependency detection methods. The results from all the methods for considered dependencies are shown in Fig.(4.6). From the results, it can be observed that p-value is consistent and precise and accurately detects the dependencies.

Even though cross-correlation slightly drops with increase in lag, still doesn't fail to detect dependencies (depends on the threshold for acceptance or rejection of dependency). Since, Pearson coefficient drops steeply from 0.75 to -0.5, correlation fails to draw any appropriate conclusion.

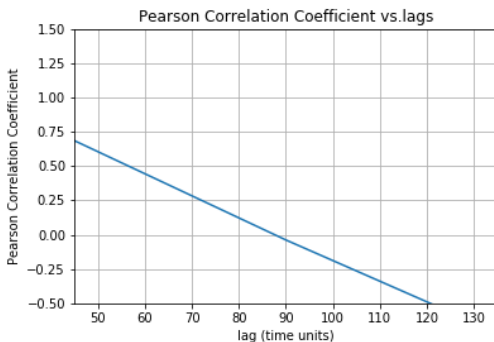
The results also show that the curves for each method remains same irrespective of the amplitudes. Hence, in this case, none of the methods are affected by the amplitude.



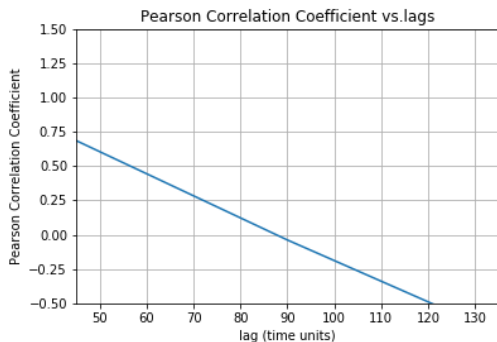
(a) p-value for the signal with high amplitude.



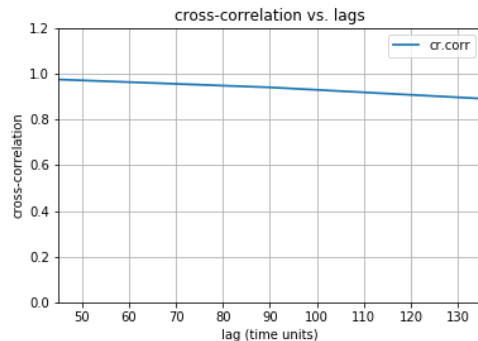
(b) p-value for the signal with low amplitude.



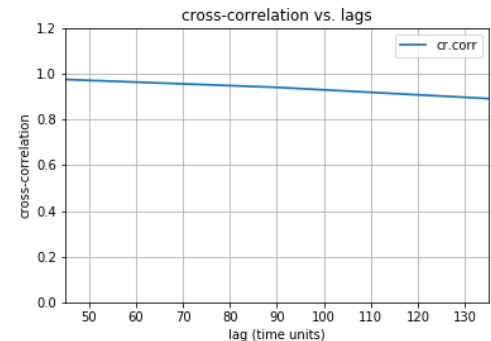
(c) Pearson coefficient for the signal with high amplitude.



(d) Pearson coefficient for the signal with low amplitude.



(e) Cross-correlation for the signal with high amplitude.



(f) Cross-correlation for the signal with low amplitude.

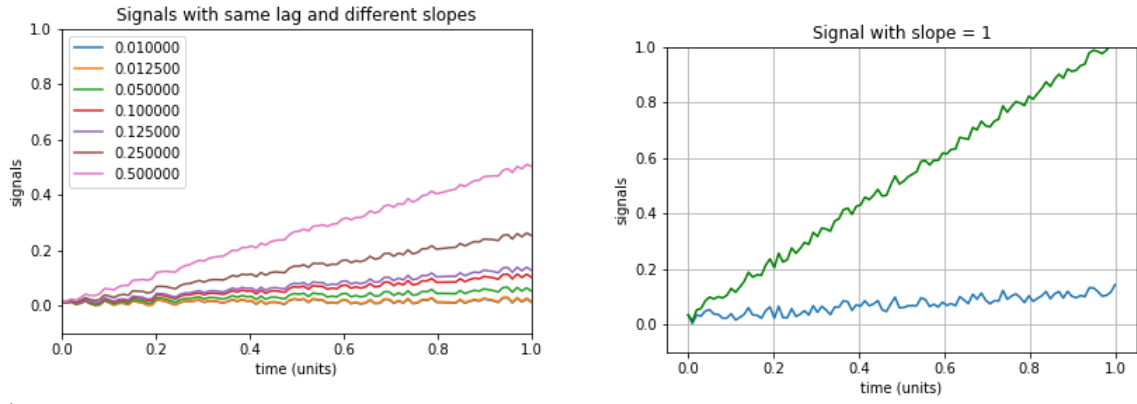
Figure 4.6: Results from all the three methods tested on the set of sinusoidal signals with different lags.

### 4.2.3 Signals with Noise

Ability to handle noise in the data is crucial for methods designed for real-time application. The sensor-dependency detection method focused here, is expected to capture dependencies from the sensors based on their data which are generally noisy, which makes it important to test the behavior of the method on noisy signals. Hence, in this section, all the three methods are tested on some noisy signals.

#### Linear Signals with Noise

This section describes the behavior of the methods on linear signals with noise.



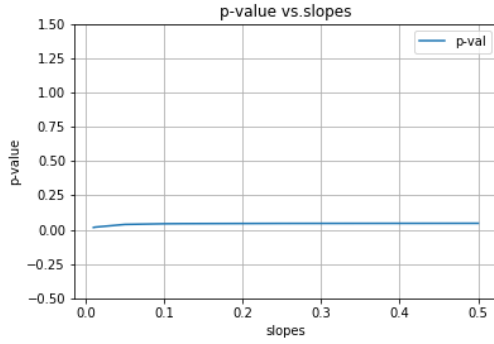
(a) Linear signals with increasing slopes with noise. (b) Noisy Linear signals to be dependent on.

Figure 4.7: Noisy linear signals with different slopes considered to analyze dependency.

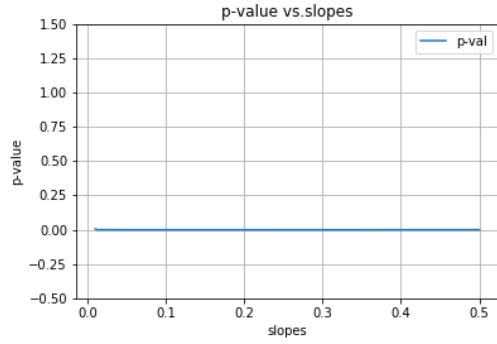
For the signals in Fig.(4.1a) and Fig.(4.1b), some uniformly distributed random noise is added to generate noisy signals with range [0,1] and [0,2] respectively. The dependency of the signals in Fig.(4.7a) on the signals in Fig.(4.7b) are tested using all the three methods.

Fig.(4.8) shows the results from all the methods for the considered signal dependencies. Granger causality, as from the results of p-value that is slightly above 0 (around 0.04) for signal with slope 0.1 (Fig.4.8(a)). However, it still indicates the existence of dependencies consistently for both signals (slope=0.1 and slope=1) even in the presence of noise.

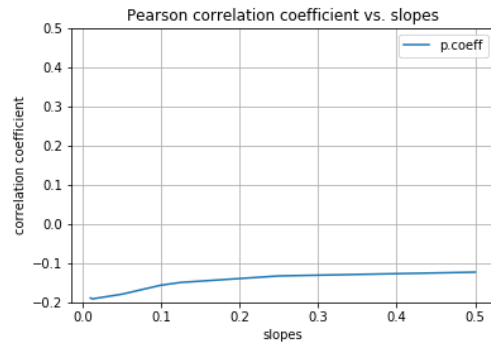
Correlation fails to detect any dependency when signal with slope=0.0001 is considered. The result is comparatively better with signal with slope=1. Hence, correlation is sensitive



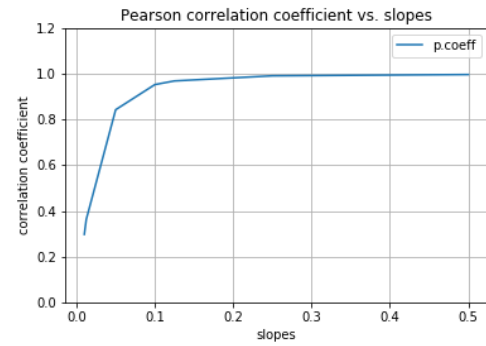
(a) p-value for the signal with slope 0.1.



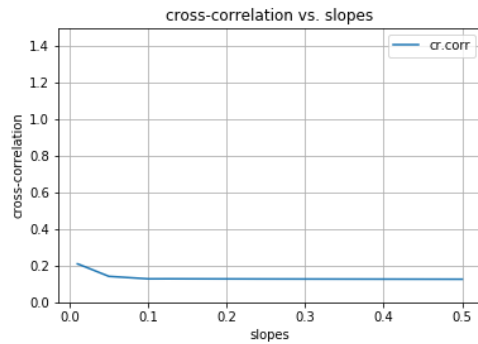
(b) p-value for the signal with slope 1.0.



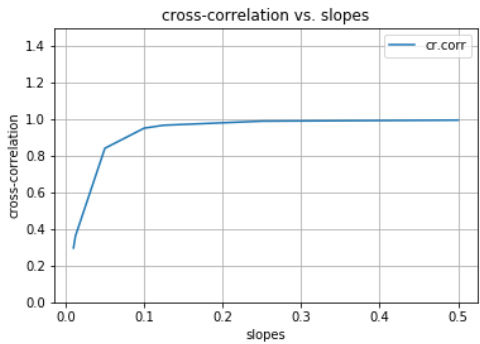
(c) Pearson coefficient for the signal with slope 0.1.



(d) Pearson coefficient for the signal with slope 1.0.



(e) Cross-correlation for the signal with slope 0.1.



(f) Cross-correlation for the signal with slope 1.0.

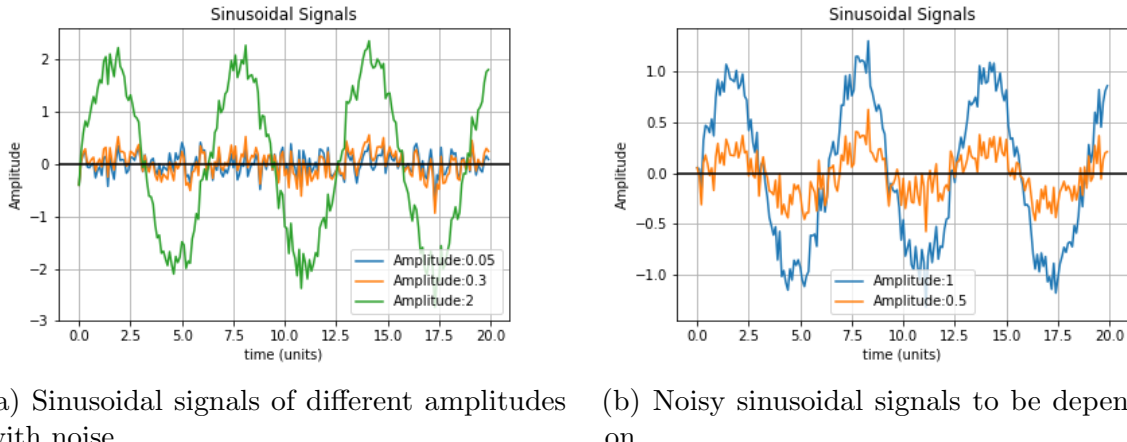
Figure 4.8: Results from all the three methods tested on the set of noisy linear signals with different slopes.

to noise as stated in [6] based on the similar analysis. In [5], sensitivity of cross-correlation to noise was discussed based on the experimental results in [4] to support the choice of Granger causality for the extension of the same work. Also from the results here, it can be observed that cross-correlation shows the behavior similar to correlation in the presence of noise.

Hence, as per observed results, Granger causality is consistent and precise in the presence of noise, compared to correlation and cross-correlation methods.

### Non-Linear Signals with Noise

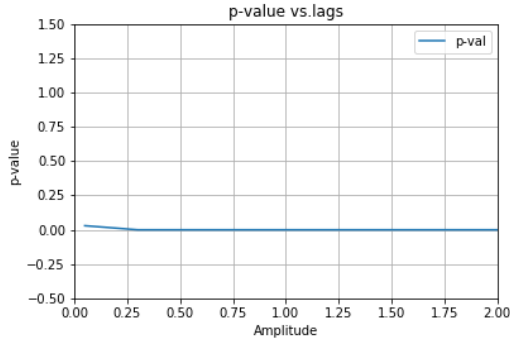
In previous section, sensitivity of cross-correlation and correlation to noise was observed. In this section same analysis is carried out on sinusoidal signals with different amplitudes. Fig.(4.9a) and Fig.(4.9b) show sine waves with different amplitudes. Some normally distributed random noise was added to make the signals noisy.



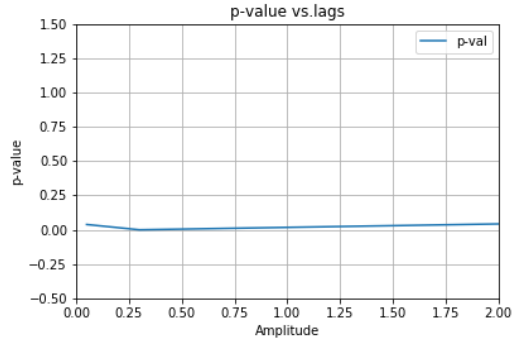
(a) Sinusoidal signals of different amplitudes  
with noise. (b) Noisy sinusoidal signals to be dependent  
on.

Figure 4.9: Noisy sinusoidal signals with different amplitudes considered to analyze dependency.

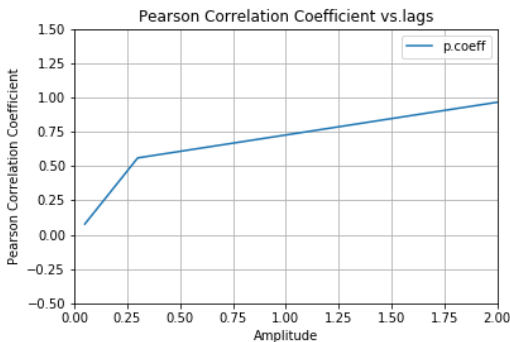
The signals from Fig.(4.9a) are expected to show dependency on the signals from Fig.(4.9b), which has comparatively has more noise. Fig.(4.9a) includes signals with very low amplitudes (amplitude of 0.05,0.3), which with noise appear to be flat signals with noise. Dependencies of these signals can be difficult to detect. The results of all the three methods are shown in Fig.(4.10). The p-value in Fig.(4.10a) and (4.10b) is slightly above zero (around 0.02) when signal with very low amplitude (amplitude = 0.05) is considered



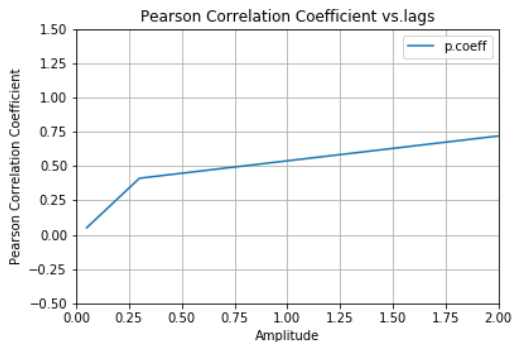
(a) p-value for the signal with high amplitude.



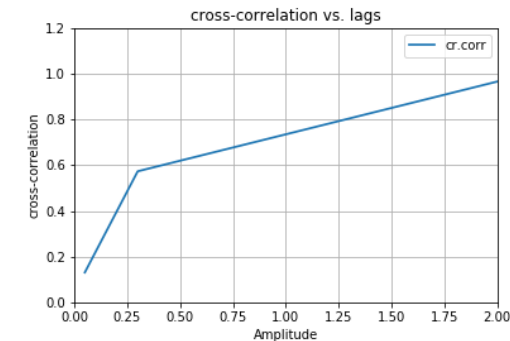
(b) p-value for the signal with low amplitude.



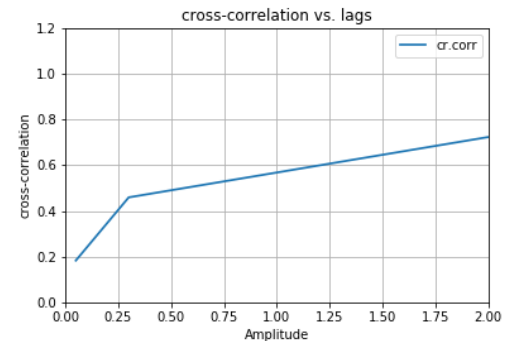
(c) Pearson coefficient for the signal with high amplitude.



(d) Pearson coefficient for the signal with low amplitude.



(e) Cross-correlation for the signal with high amplitude.



(f) Cross-correlation for the signal with low amplitude.

Figure 4.10: Results from all the three methods tested on the set of noisy non-linear signals with different amplitudes.

to detect dependency. Also, in (4.10b), the curve of p-value is above zero (around 0.04) , when high amplitude signal (amplitude = 2.0) is compared against comparatively low amplitude signal (amplitude = 0.5).

Pearson correlation coefficient value is very low for low amplitude (0.05) in both cases as shown in Fig.(4.10c) and Fig.(4.11a). When signal with high amplitude (2.0) is checked for dependency on low amplitude signal as shown in Fig.(4.11a), performance is reduced from that in Fig.(4.10c) as Person coefficient value drops from close to one to 0.75. Cross correlation also shows same behavior as correlation for both the cases. It can be observed that the amplitudes of the signals affect dependencies when same amount of noise is added to the signals with different amplitudes. Also, the results confirm that Granger causality is more robust to noise than other two methods.

### 4.3 Granger Causality on Sliding Window

In sensor-based fault detection and diagnosis implemented in [27], input is provided to the algorithm in a sliding window fashion. The window is a  $m \times n$  matrix where  $m$  denotes sensor data for  $m$  time units and  $n$  is the number of sensors. The window can be functionally divided into two parts, where first half is dedicated to note the dependency patterns and second half tests whether the patterns persist or are violated. If dependency is violated in the second half due to suspicious pattern shown by any of the sensors, the sensor is assumed to be faulty. This is the setup to detect faults on line, and diagnose it as fast as possible.

As mentioned earlier, [27] used correlation for dependency detection. In the extended work [6], the practical considerations in implementation of SFDD with correlation was discussed and it was shown that size of the window and noise play crucial role in the performance of correlation.

In this section, the signals are generated as in [6], and are used to determine the performance of Granger causality on sliding window.

#### 4.3.1 Effect of Window Size on Granger Causality

The delay in response of correlation due to window size was discussed in [6]. For the similar set of signals, Granger causality is implemented and is compared with correlation.

This comparison can be seen in Fig.(4.11). Ideally, the signals are expected to be dependent throughout except at the points where signal 1 shows sudden changes.

The signals considered show windowed dependencies. Some uniformly distributed random noise in the range [0,0.05] are added to both the signals. Pearson correlation coefficient and p-values are plotted with window size of one time unit and two time unit to analyze the response.

Granger causality also has a delay with window size as correlation. Also, like correlation, the increase in window size results in more stable response.

As discussed in [6], correlation does not show any visible response on discontinuities in the signal. This holds good on Granger causality as well, as sudden changes cannot be predicted through the p-value curve in Fig.(4.11c) and Fig.(4.11d).

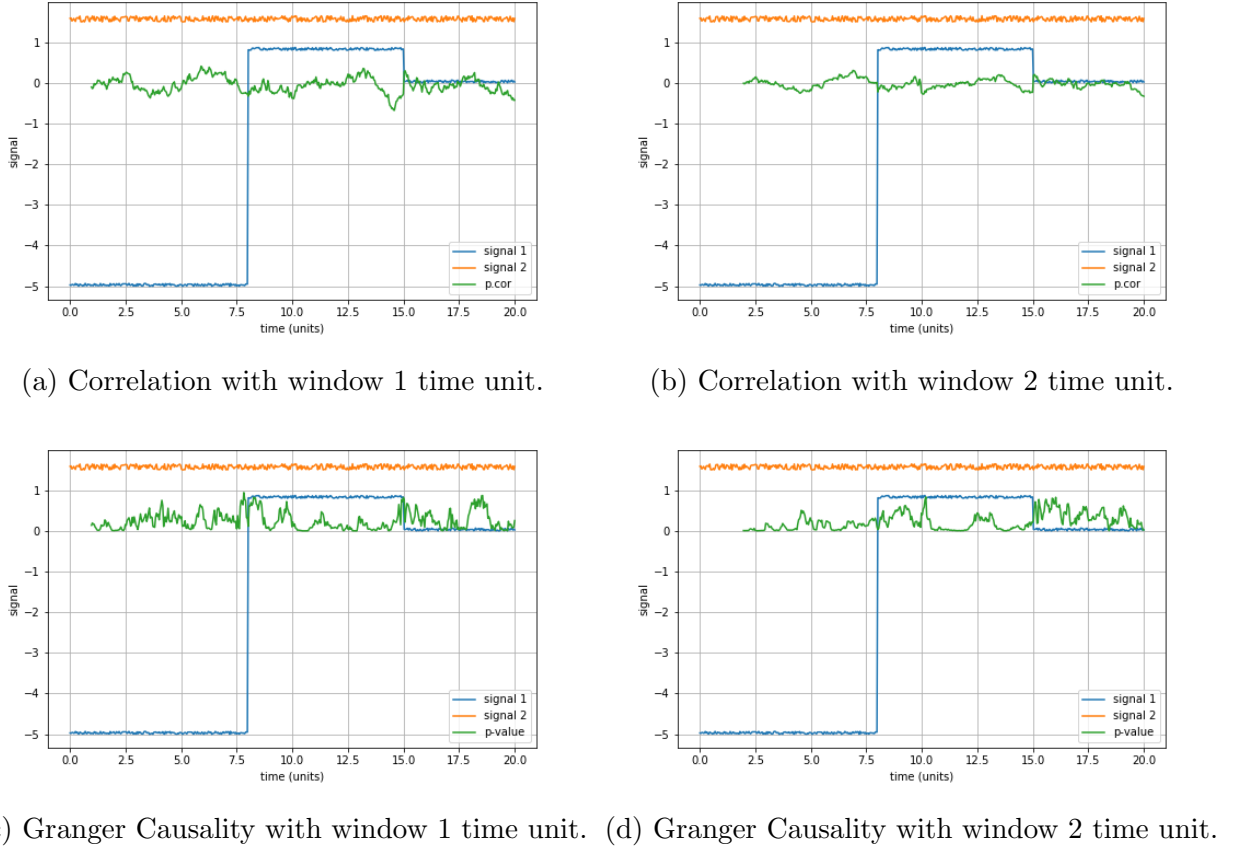
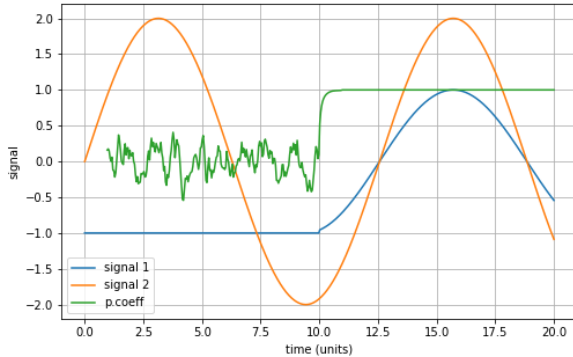


Figure 4.11: Delay in response of Pearson coefficient and p-value due to window size.

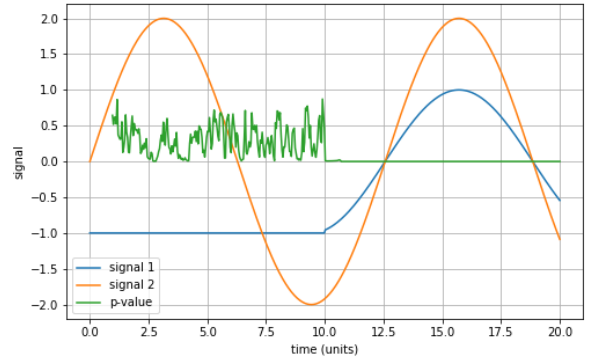
### 4.3.2 Effect of noise on Granger Causality

In the previous section, robustness of Granger causality to noise was observed considering complete data at once. But, handling the noise in data on sliding window can be comparatively difficult as inherent structure of the data is not known. In this section effect of noise on Granger causality with sliding window is analyzed.

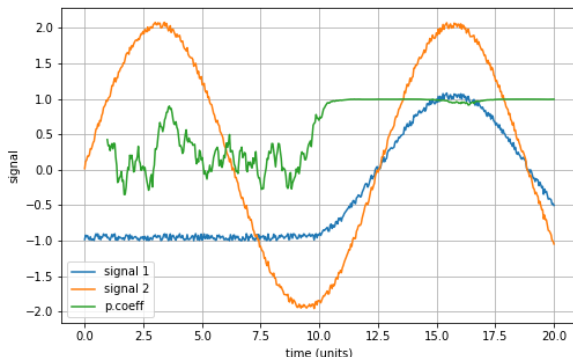
The signals considered exhibit windowed dependency. The signals are partly dependent as shown in Fig.(4.12) i.e the signals are not dependent in the first half and are dependent in the second half of the plot. Hence, a dependency detection method is expected to detect dependency in the region where dependency exists. However, noise in the data would not allow ideal response of the method.



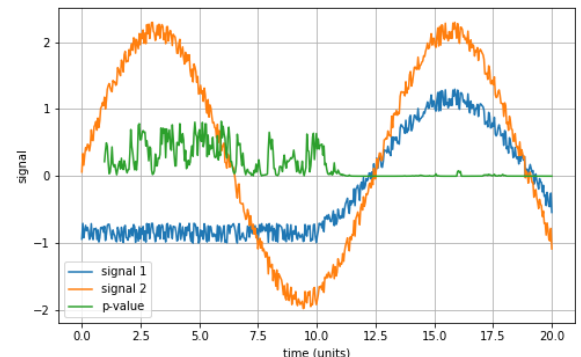
(a) Correlation with window 1 second



(b) Granger Causality with window 1 second



(c) Correlation with window 1 second



(d) Granger Causality with window 1 second

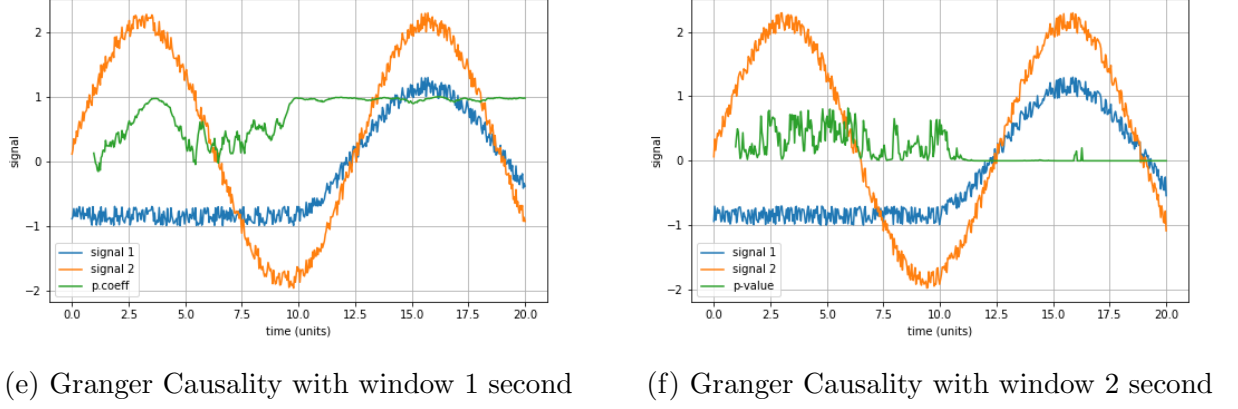


Figure 4.12: Delay in response of Pearson coefficient and p-value due to window size.

In this case, Granger causality is implemented on the signals with window size of one time unit. It is compared with correlation with same window size and noise. In [6], degradation of performance of correlation with noise is shown. From Fig.(4.12), it can be observed that performance Granger causality degrades with noise as well. In both the cases, though the existence of dependency is indicated precisely, the non-existence of dependency is not acceptably clear.

### 4.3.3 Effect of Changing Frequencies on Granger Causality

In this case, signals with changing frequencies are considered on a sliding window of size 0.2 second. A small Gaussian noise ( $\mu = 0, \sigma = 0.05$ ) is added to both the signals with different amplitudes (0.5,1). Although both Granger causality (shown in Fig.(4.13b)) and correlation (shown in Fig.(4.13a)) appear to behave well with the noisy signals with changing frequencies (with p-value=0, Pearson-coefficient close to 1), Granger causality, evidently is more precise and consistent as compared to correlation.

From the curve in Fig.(4.13a), it can be seen that Pearson coefficient is not consistently 1 for curves with lower frequencies. The consistency and accuracy of correlation increases with the frequency of the signals. On the other hand p-value does not vary with frequencies even in the presence of noise. Hence, from the result, it can be concluded that both the methods, especially Granger causality behaves well with changing frequencies on sliding window of very small size.

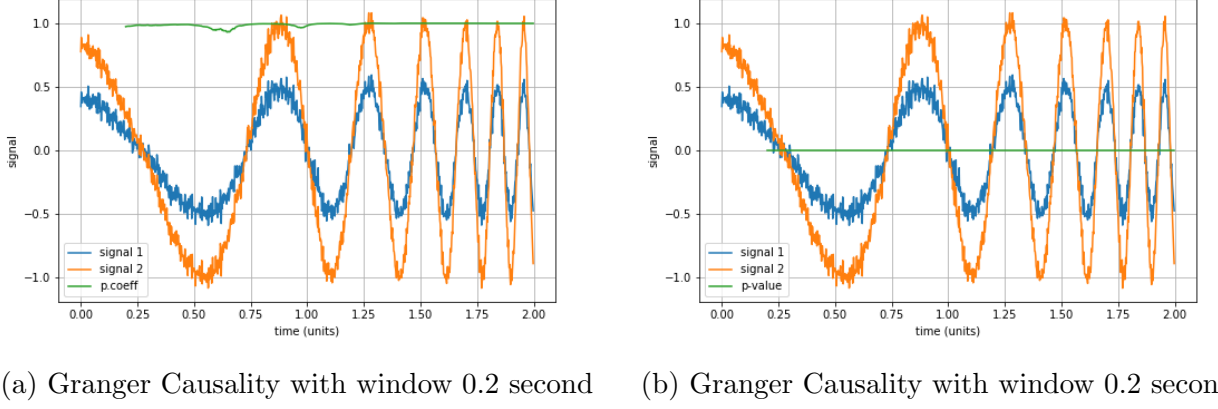


Figure 4.13: Delay in response of Pearson coefficient and p-value due to window size.

#### 4.4 Comparison of Granger Causality with other methods

Granger causality, as described before, detects Granger causal relationship. Hence, comparing Granger causality with correlation and cross-correlation on same set of signals may not make perfect sense. However, in the correlated signals considered in section 4.2, one signal was able to predict the other. This may not be true for all correlated data. It is possible for Granger causality to not exist in highly correlated data. For example, if two signals are identical, the past values of the signals are also identical, which do not add any information for prediction of future values of the other signal.

This difference of Granger causality from correlation can make it less intuitive. Specifically, correlation can be approximated between signals intuitively based on the redundant information available from a system. This can also hold for cross-correlation when two signals are correlated with a lag. But, this is not true for Granger causality. Also, Granger causality provides directed relationships unlike correlation and cross-correlation.

One of the important reasons that supports feasibility of Granger causality is the difficulty in determination of threshold in correlation and cross-correlation. Threshold value below which dependency is accepted or rejected, plays crucial role in fault detection. A standard threshold (0.05 p-value) is used in statistics for Granger causality. Hence, a confidence level and dataset is sufficient to implement Granger causality. Moreover, the results from the section 4.2 show that Granger causality performs better than cross-correlation and correlation in most of the cases, especially in presence of noise and lag.

# 5

## Evaluation

This chapter describes the system considered for the evaluation of proposed solution. Further, a brief description of experimental design and intuition behind designed experiments for the evaluation is given.

### 5.1 Hardware Setup

In this section, hardware setup of the system and the intuition behind using this system is explained in detail.

#### 5.1.1 Overview - The Ropod Platform

The ropod is an Automatically Guided Vehicle for logistic applications, developed as a part of the ROPOD project<sup>1</sup>. This ropod platform (figure 5.1a) consisting of four smart wheels (robotic pods) is used to evaluate proposed solution for dependency detection. The strict modular structure of the ropod platform makes it suitable for decomposition of the system into a structural model, providing a natural hardware framework for the dependency detection problem, that aims to satisfy structural model-based approach for fault detection.

Although the experiments are conducted using an entire platform, on different scenarios, proposed solution can be applied at subsystem levels for the better analysis of working of the solution. Each smart wheel, comprising of twin-wheels in a differential drive

---

<sup>1</sup><http://www.ropod.org/>



(a) The ropod platform



(b) Smart wheel

Figure 5.1: The ropod platform with four smart wheels consisting of twin-wheels (figure 3.1b taken from preliminary results of the original project [http://www.ropod.org/preliminary\\_results.html](http://www.ropod.org/preliminary_results.html))

configuration Fig.(5.1b), can be viewed as an individual system consisting of various sensors and actuators. Hence, if the platform is used to generate various motion patterns, data from one wheel can be considered to test the solution, making analysis of the performance of proposed solution relatively easy.

### 5.1.2 Sensors in Ropod Smart Wheel

Each of the ropod smart wheel units comprises of twin-wheels, with in-wheel motors, each provided with an encoder. The 3-phase BLDC motors are arranged in a differential-drive configuration with a castor offset. The encoders are used to obtain absolute position of the twin-wheels. Also, a pivot encoder is positioned to measure orientation of the wheels. An on-board IMU sensor and a temperature sensor is also present in the unit. A smart wheel controller is used to drive the motors and to process information from the sensors. Figure 5.2 shows a schematic diagram of the smart wheel components. In addition to the main sensors (i.e three encoders and an IMU), there are current and voltage variables that are sensed internally, and their values can be accessed.

As dependency detection primarily exploits spatial and temporal relationships between the sensors, it is important to know the information provided by each of the sensors. Any obvious relationship/redundancy existing among sensors can thus be recognized easily. Further, it can also be used to draw functional relationships among the sensed variables. In addition to the variables that are physically sensed, few derived variables from the

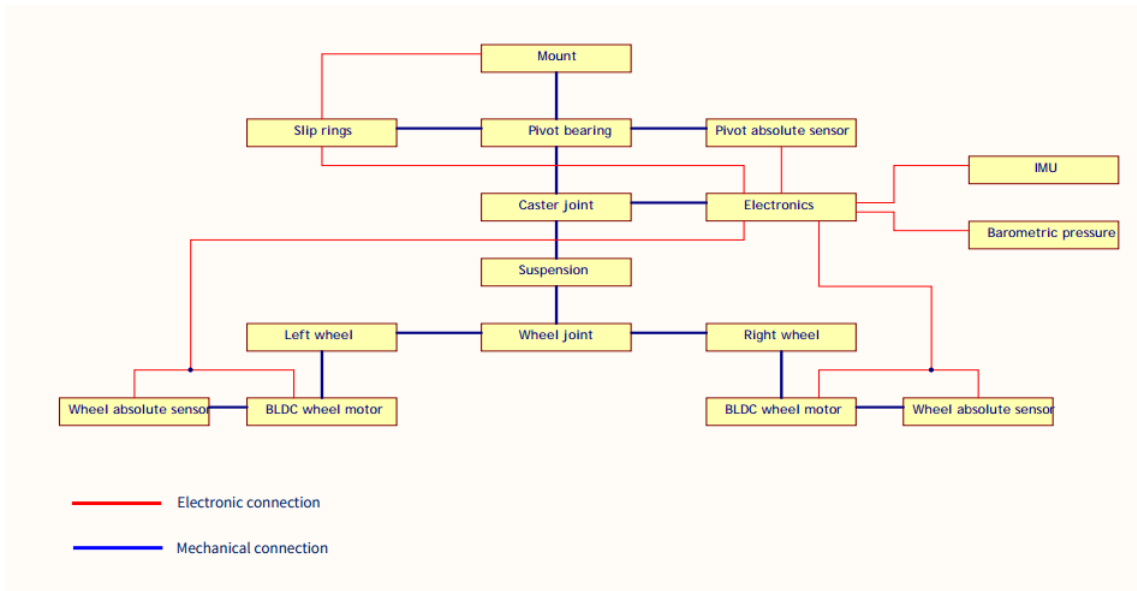


Figure 5.2: Schematic representation of smart wheel components (taken from design documents provided by Speciaal Machinefabriek Ketels VOF, Copyright of A. Ketels, 2017)

sensed information are also provided.

All the sensors available on a smart wheel is listed with corresponding sensed and derived variables in table 5.1.

## 5.2 Experimental Design

The experiments designed to evaluate implemented method should be able to assess its ability to detect the expected dependencies in various scenarios when the system appears to exhibit normal behavior. Since, the existence of all the expected dependencies depict no fault in the system, if at any time, the system stops exhibiting normal action, at least one relevant violation of dependency should be recognized from the method to indicate fault in the system. Hence, the experiments are designed such that:

- All existing dependencies that the method aims to find are detected.

## 5.2. Experimental Design

---

Sensors	Sensed Variables	Units(Symbol)	Variable Names	Derived Variables	Units(Symbol)	Variable Names
Wheel encoders	Position of the twin-wheels	rad	encoder_1 encoder_2	Velocity of the wheels	rad/s	velocity_1
Pivot encoder	Orientation of the twin-wheels	rad	encoder_pivot	Velocity of the pivot	rad/s	velocity_pivot
IMU	Acceleration in x-axis	m/s <sup>2</sup>	accel_x			
	Acceleration in y-axis	m/s <sup>2</sup>	accel_y			
	Acceleration in z-axis	m/s <sup>2</sup>	accel_z			
	Rotation in x-axis	rad/s	gyro_x			
	Rotation in y-axis	rad/s	gyro_y			
	Rotation in z-axis	rad/s	gyro_z			
Current sensor	Current U	A	current_1_u	Quadrature current	A	current_1_q
	Current V	A	current_1_v			voltage_1
	Current W	A	current_1_w			current_1_d
			current_2_u	Voltage equivalent to quadrature current	V	current_2_q
			current_2_v	Direct Current	A	voltage_2
			current_2_w			current_2_d
Voltage sensor	Bus/Battery Voltage	V	voltage_bus	Voltage U	V	voltage_1_u
				Voltage V		voltage_1_v
				Voltage W		voltage_1_w
Temperature sensor	Temperature of IMU	K	temperature_imu			voltage_2_u
Pressure sensor	Barometric pressure	Pa	pressure			voltage_2_v
						voltage_2_w

Table 5.1: Table listing all the sensors available on a smart wheel with two wheels with a 3-phase BLDC motor each, along with corresponding sensed and derived variables with units.

- When a known fault is injected in the system, at least one dependency should be violated and possibly, the reason behind the violation should be justifiable as per working of the method.

To test if these criteria are satisfied, the experiment is designed in the following regards for each above mentioned criterion respectively.

### 5.2.1 Generating Different Motions with The Ropod Platform

For all the sensor dependencies to be detected, it is crucial to run the system in all possible ways, so that all the sensors in the system prove their relevance and exhibit their relationships with other sensors. This holds a fundamental importance with the fact that not all sensors are triggered to the same extent by the system in all execution states, and the dependencies exhibited may vary with the mode of action.

Considering the ropod platform, if it is run for a straight line forward motion, the orientation of the robot doesn't change with time, and hence, pivot encoder values remain constant. However, when the motion is an arc to the left/right, the pivot encoder values are not constant anymore and may exhibit some relationship with wheel encoders. Thus, experimenting with different motions such as: straight line ahead, an arc to the left/right, on spot rotation gives a better judgement on the working of the method.

In addition to this, to better analyze the solution, the experiment can be conducted in both torque and velocity modes. Also, testing at varying velocity helps to keenly observe its dependency with current variables.

### 5.2.2 Injecting Faults into the System

As sensor dependencies are detected for the purpose of fault detection, it is important to test the method when system is faulty. This allows the comparison of normal and abnormal behavior. The dependencies drawn from various motions as discussed earlier can be compared against the dependencies that a faulty system provides for similar motions. To do so, known faults can be injected so as to recognize the violation of dependencies that are expected to be violated.

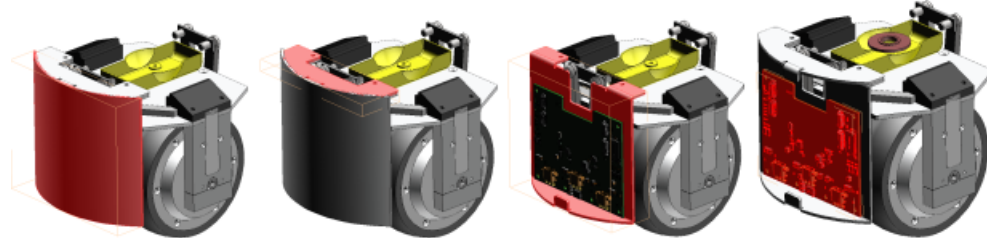


Figure 5.3: Electronics cover of smart wheel removed (taken from the CAD drawings by Speciaal Machinefabriek Ketels VOF)

In this case, the sensor wires can be unplugged to induce abnormal behavior in to the system. This is not only a simple way to inject fault, but also indicates the clear violations of dependencies. The intuition behind this is that when a sensor is unplugged during execution, its related sensors still continue to work and since there is change in

dependency and unplugged sensor exhibits a susceptible pattern (section 1.2.2), a fault has to be indicated.

The cover of circuit board for smart wheel can be removed as seen in the figure 5.3. This provides access to the wheel encoders, pivot encoder and power supply for the wheel. The sensors are connected as shown in the figure 5.4. All these sensors for a wheel can be unplugged one at a time, and the system can be run for all motions discussed above. This helps in observing the affect of removing each sensor in the system and ideally, the sensors associated with the unplugged sensor will no more exhibit relationship with it. This deviation from the nominal set of dependencies can further be used for fault detection.

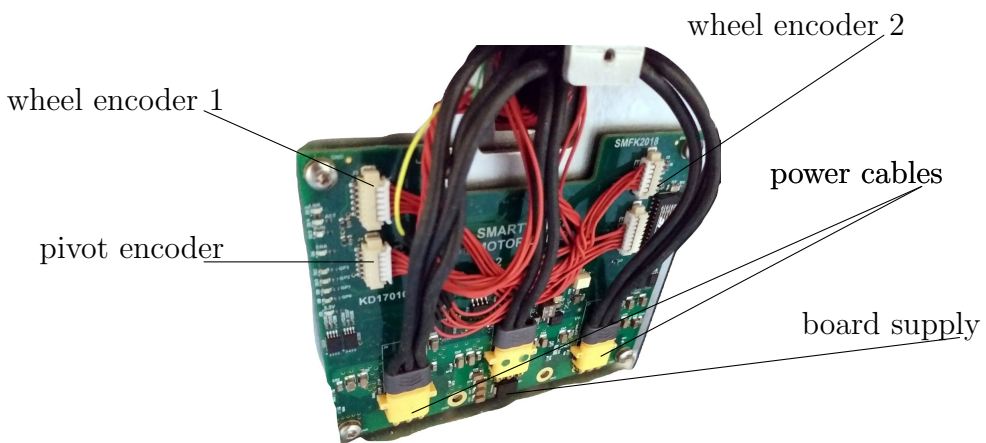


Figure 5.4: Circuit board for ropod smart wheel

Thus, the performance of the dependency detection method proposed in this work can be evaluated effectively.

### 5.3 Evaluation Procedure

- To evaluate Granger causality using the ropod platform, motions are generated using the whole platform.
- For every motion, different faults are injected to analyze the performance of the method on faulty data.

- For actual evaluation, the data from only one smart wheel is considered, as it makes a whole system by itself as mentioned in section 5.1.1.
- For every set of data from each motion, p-values are generated. In the given confidence interval (1 sigma Gaussian interval), the least available p-value that corresponds to highest F-value is considered as the best p-value.
- These p-values are used to interpret dependencies, i.e if p-value is  $\leq 0.05$ , dependencies are considerable if not, no dependency exists.
- The p-values denoting dependencies for nominal and faulty cases are compared.
- For a couple of variables among which dependencies are violated with faults, the change of p-value is observed by evaluating signals on sliding window. To do so, separately collected nominal and faulty data are concatenated at a point, to make the data appear to have fault injected in middle of the normal execution.
- The injection of fault is expected to violate Granger causal dependencies existing in nominal execution state, which should trigger change of p-values.
- The response of p-values on sliding window is used to analyze the real-time performance of Granger causality.

---

### 5.3. Evaluation Procedure

# 6

## Experimental Results

This chapter analyses the results from the experiments conducted on the ropod platform to evaluate the performance of dependency detection using Granger causality. As mentioned earlier, the evaluation of a smart wheel of the platform is considered in every case. The experiments are conducted in two different modes i.e torque, velocity. For each mode, the results from nominal and fault injected cases are explained.

### 6.1 Evaluation in Torque Mode

The ropod platform is remote controlled in torque mode. The velocity hence, is not constant. The variables 'setpoint 1' and 'setpoint 2', the setpoint modes of the platform, set current (in amp) as per the remote commanded velocities. In this section, the results from the experiments in torque mode are analyzed for various motion patterns.

#### 6.1.1 Defining Dependencies for Nominal Motions

In this section, the dependencies in nominal execution mode, for different motions are defined. This provides a general idea of the dependencies associated with sensor variables. These dependencies provide a reference for further evaluation of fault injected behavior. In other words, if a sensor having a dependency with another sensor is subjected to fault, the violation of the dependency between them indicates the fault. The ropod platform is moved to generate straight, and smooth curves towards left and right motions using a remote. In addition to these, the platform is rotated on spot in both clockwise and

## 6.1. Evaluation in Torque Mode

anti-clockwise directions. The data of sensed variables for each nominal motion is recorded for all the wheels. However, for all the directly sensed variables, the p-values are generated using Granger causality for one considered wheel. Fig.(6.1) shows the set of p-values for pairs of variables with the direction of causality going from x axis to y axis i.e variables in x-axis cause variables in y-axis. Although the matrix appears like a confusion matrix, it is not interpreted as such.

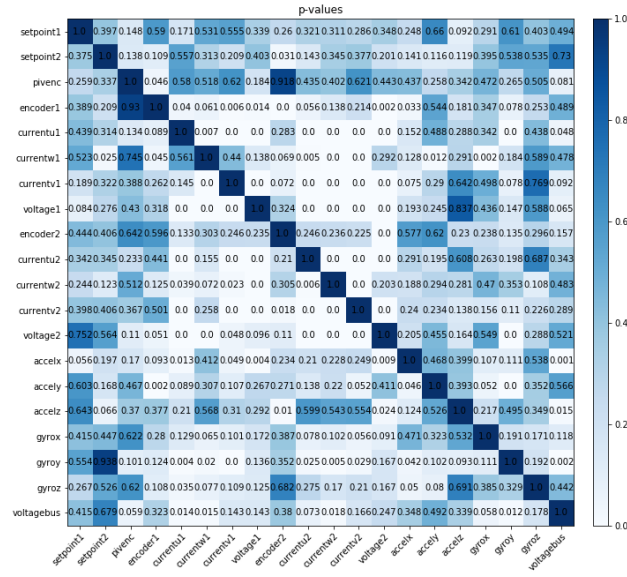


Figure 6.1: Granger causal dependencies defined by p-values for nominal straight motion with lighter shades indicating dependencies.

The lighter the shade of the box, the stronger the dependency, with lesser p-value. Dependencies exist between two variables when  $p\text{-value} \leq 0.05$ . The dark shade of the diagonal elements ( $p\text{-value}=1$ ) indicate no dependency between the variables with themselves. This is reasonable because the variables already have their past values and they do not need the same past values from their replicated signals for the better prediction of their future values. Similarly, the p-values for nominal curve and on spot rotation motions are shown in Fig.(6.2) and Fig.(6.3) respectively.

These figures for nominal states are used as reference to check the change in p-values when any fault is induced. All the faults are induced on the same wheel for which nominal dependencies are defined. As long as the indication of p-values (causal or not) is same as

## Chapter 6. Experimental Results

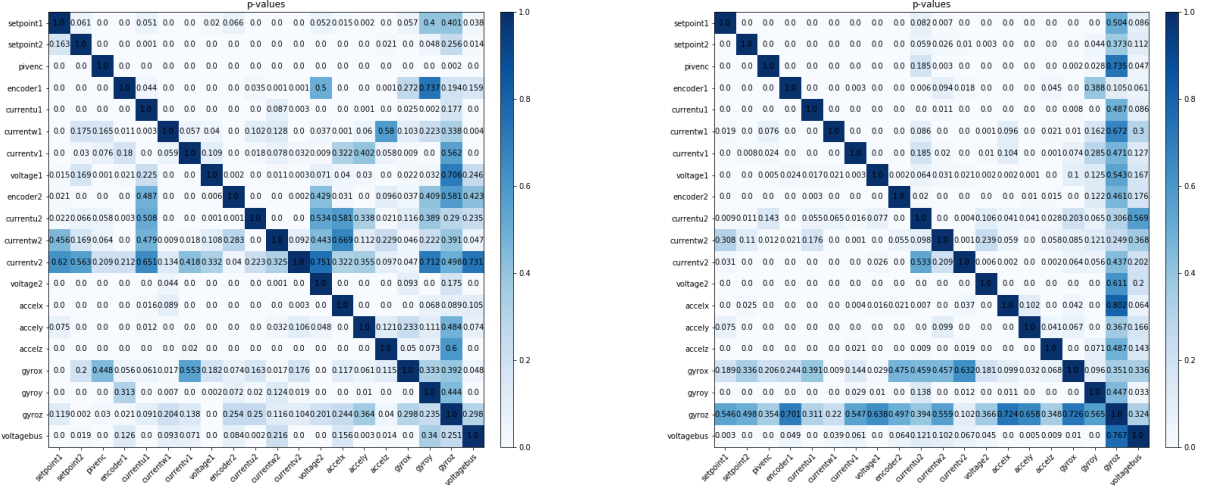


Figure 6.2: Granger causal dependencies defined by p-values for nominal curved motions.

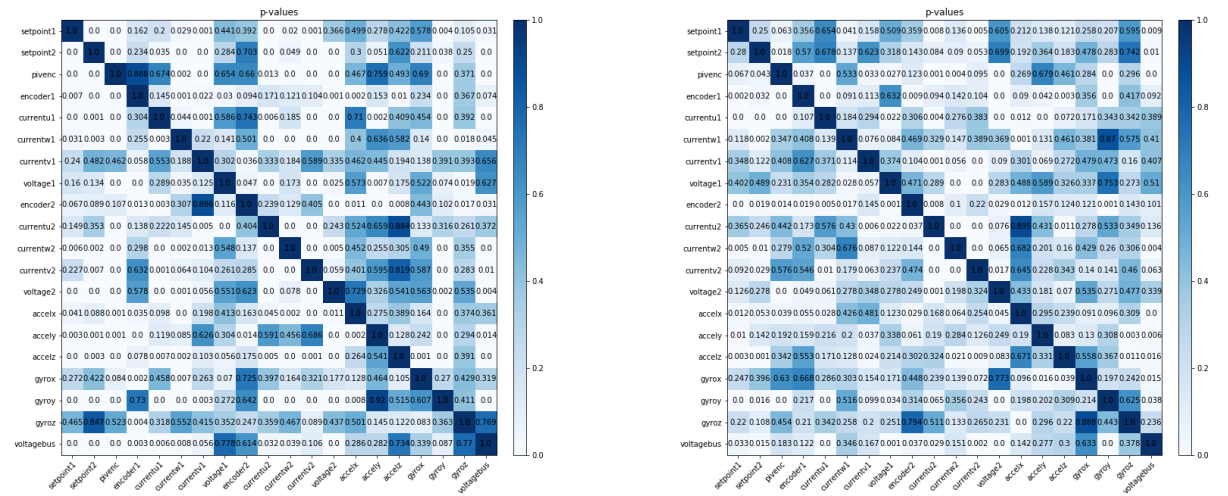


Figure 6.3: Granger causal dependencies defined by p-values for nominal on spot rotations.

## 6.1. Evaluation in Torque Mode

the nominal ones for the sensed variables, the variables are considered to be normal. This helps to test behavior of Granger causality when fault is induced.

### 6.1.2 Dependency Detection with an Unplugged Wheel Encoder

To analyze how p-value changes, in turn changing the dependencies, on abnormal behavior in the system, faults are injected into the system. In this section, the results of Granger causality for all the motion patterns are analyzed with the wheel encoders unplugged one at a time. Every smart wheel is a set of two wheels and has one encoder on each of the wheels. The encoders are referred as 'encoder 1' and 'encoder 2' in rest of the chapter.

#### Straight Motion

The straight motion of the ropod platform is generated by unplugging the encoders of a smart wheel, one at a time. The p-values obtained with each encoder unplugged is shown in Fig.(6.4a) and Fig.(6.4b).

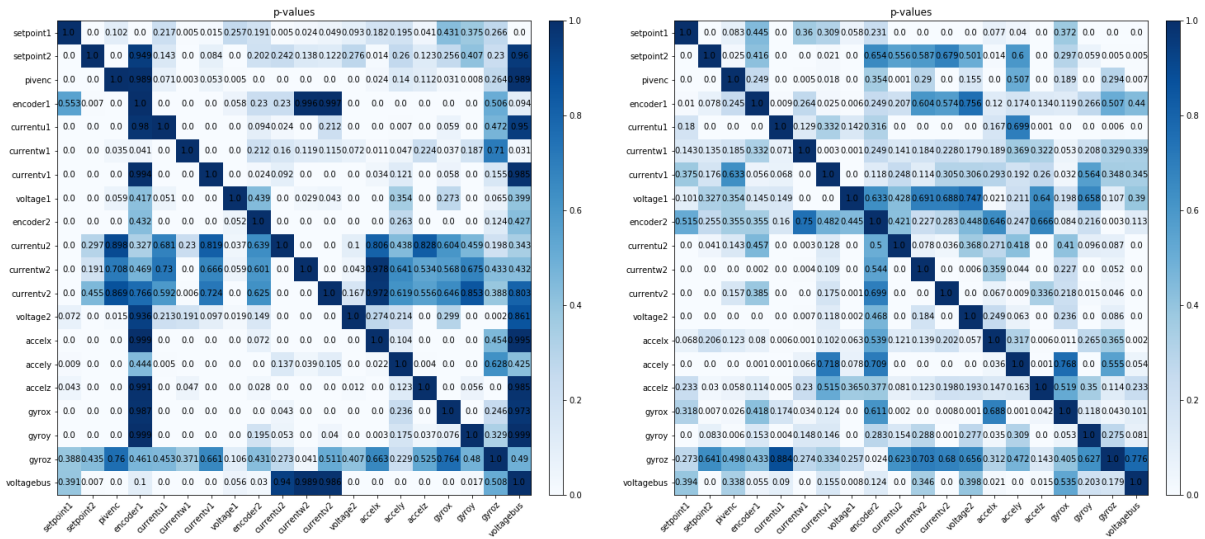


Figure 6.4: p-values for straight motion with unplugged encoders.

To provide clear idea on dependencies associated with encoder 1 and 2, dependency diagrams are generated as shown in Fig.(6.5). The Fig.(6.5a) and Fig.(6.5c) are for nominal straight motion, as defined in Fig.(6.1). The Fig.(6.5b) and Fig.(6.5d) are for encoder 1 and encoder 2 unplugged conditions respectively as defined in Fig.(6.4).

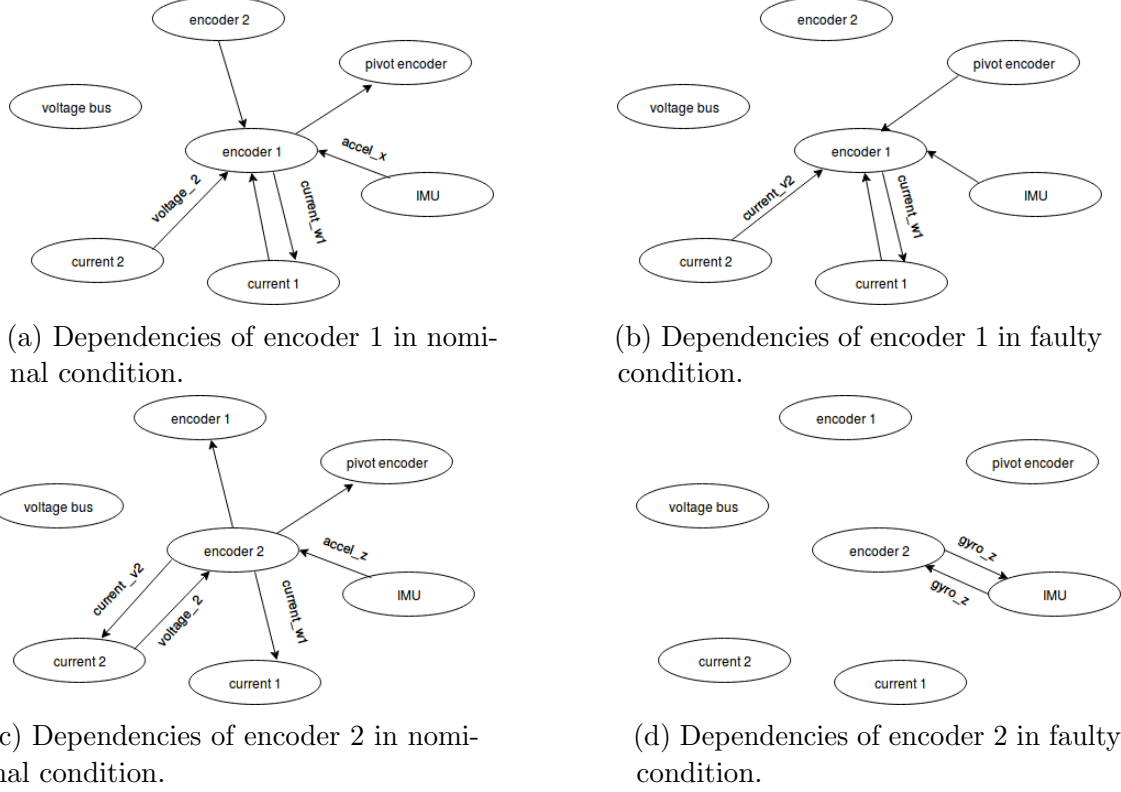


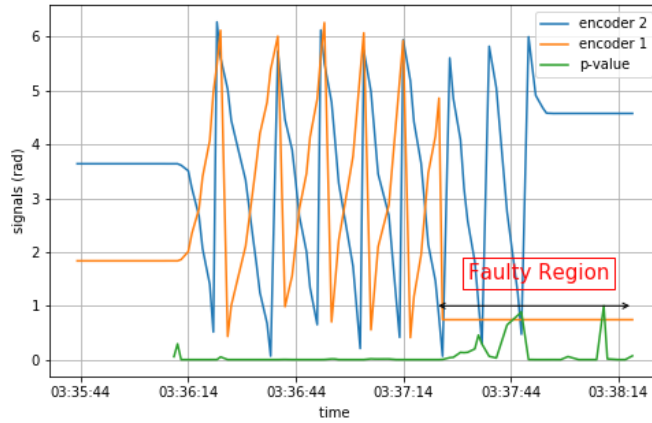
Figure 6.5: Granger causal dependency diagrams for encoder 1 and 2 in nominal (left column) and faulty (right column) conditions in straight motion.

The dependency diagrams have unidirectional arrows from the variable causing to variable caused. For example, in Fig.(6.5a), encoder 2 causes encoder 1. The variables current 1 and current 2 indicate current sensors for each wheel and voltage bus is the voltage sensor. The variables with the arrows indicate the variable sensed by the sensor that is caused/causing. If no variable is with the arrow, that indicates all the variables associated with the sensor are causing/caused. In Fig.(6.5a), arrow from current 2 to encoder 1 with voltage 2 indicates voltage 2 variable associated with current 2 sensor is causing encoder 1.

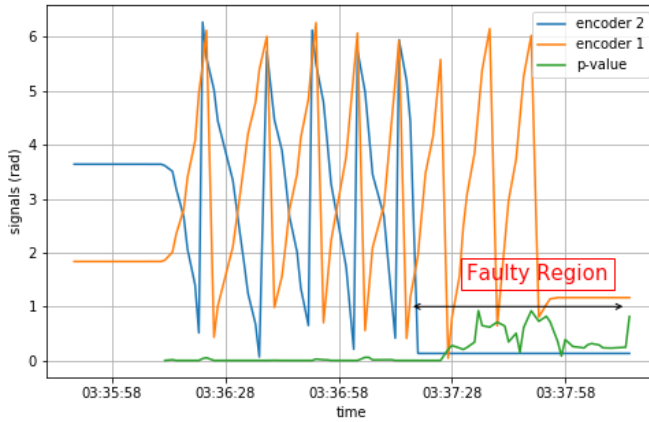
## 6.1. Evaluation in Torque Mode

From the Fig.(6.5), it can be observed that with fault induced, most nominal dependencies disappear and few additional dependencies are generated. When the change in this pattern happens, the fault is expected to be detected. Considering that, when encoder 1 and 2 are unplugged, the Granger causality from encoder 2 to encoder 1 disappears, the dependency detection for this case is performed on a sliding window.

In section 4.3, the purpose of sliding window was discussed. The change in the p-value when fault is induced is hence tested on a sliding window.



(a) Change in p-value when encoder 1 is unplugged.



(b) Change in p-value when encoder 2 is unplugged.

Figure 6.6: Change in p-value when fault is introduced by unplugging encoders.

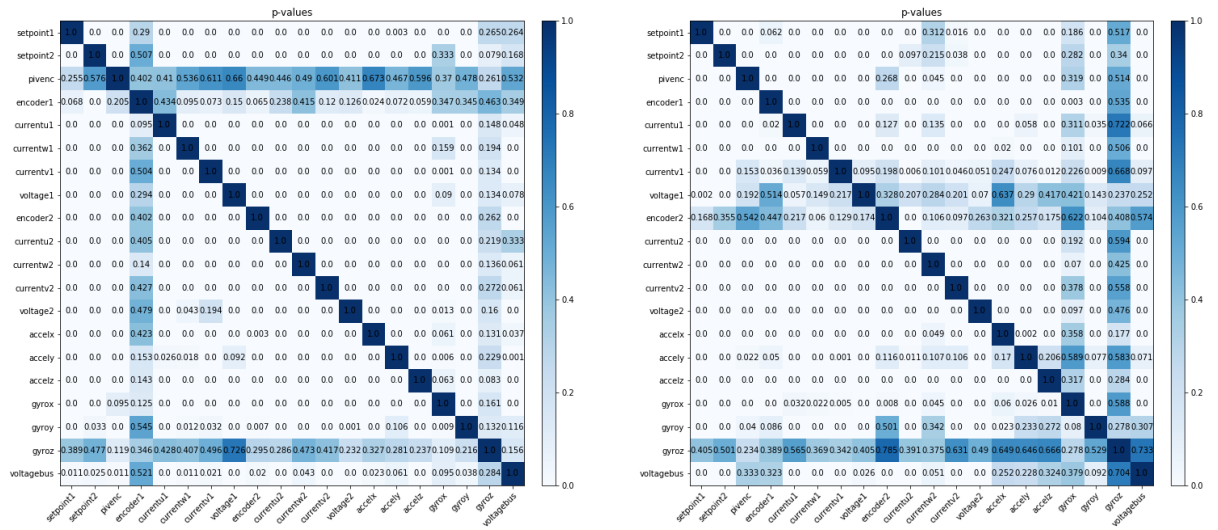
## Chapter 6. Experimental Results

---

The p-value on sliding window with window size 1.5 second is shown in Fig.(6.6). When the data is normal p-value is very close to zero indicating high Granger causal dependencies between the signals. When the signals enter faulty region, i.e when one of the encoders are unplugged, the corresponding signal shows 'stuck' pattern. The p-value crosses the threshold in this region. Hence, Granger causality indicates the violation of dependency in this case.

### Curved Motion Left

For the same fault in the encoders as defined in the previous section, the dependency detection method is evaluated here for a smooth curved motion in the left direction. The p-values generated for the cases of unplugged encoder 1 and encoder 2 in curved left motion is shown in Fig.(6.7).



(a) Curved left motion with encoder1 unplugged.

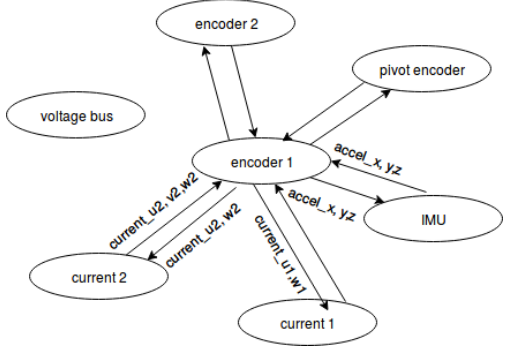
(b) Curved left motion with encoder2 unplugged.

Figure 6.7: p-values for curved left motion with unplugged encoders.

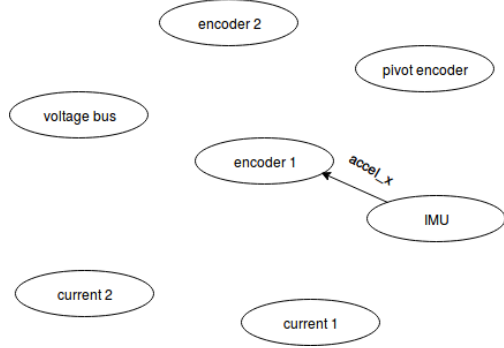
The dependency diagrams for encoder 1 and 2 in nominal and faulty cases are shown in Fig.(6.8). In Fig.(6.8), it can be observed that when encoder 1 is unplugged, the Granger causality between encoder 1 and encoder 2 in both directions disappear and when encoder

## 6.1. Evaluation in Torque Mode

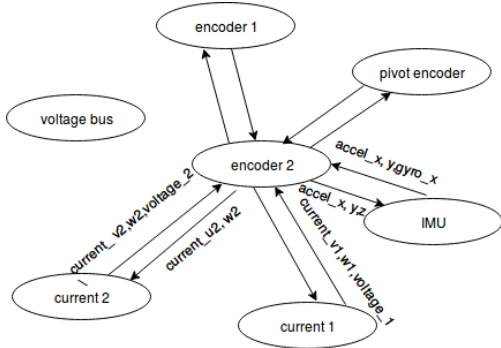
2 is unplugged, Granger causality from encoder 2 to encoder 1 disappears. Also it can be observed that, encoder 2 when unplugged, retains more dependencies as compared to encoder 1.



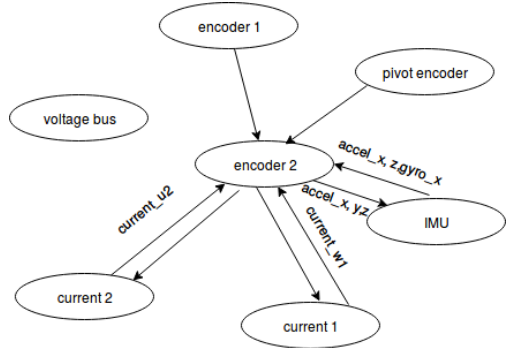
(a) Dependencies of encoder 1 in nominal condition.



(b) Dependencies of encoder 1 in faulty condition.



(c) Dependencies of encoder 2 in nominal condition.

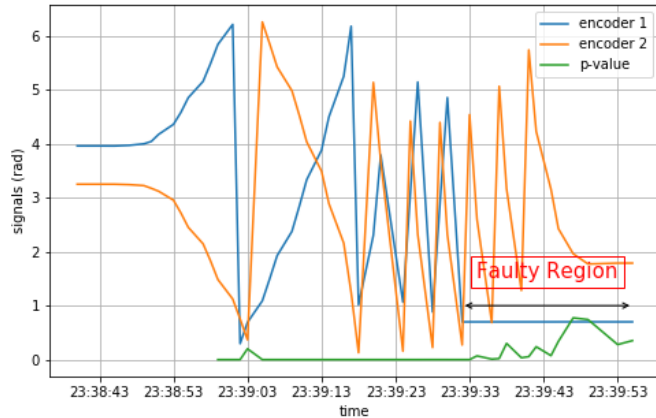


(d) Dependencies of encoder 2 in faulty condition.

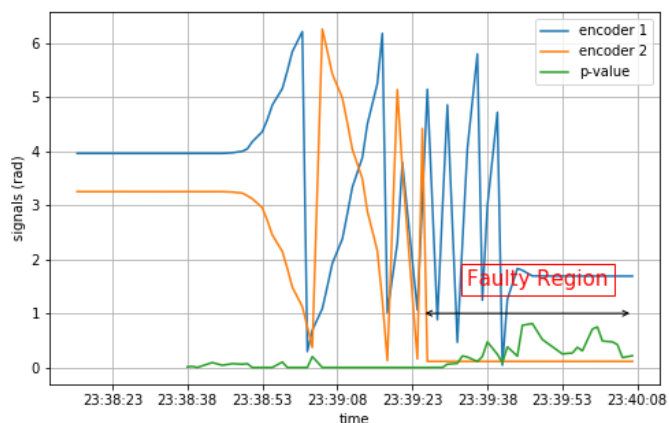
Figure 6.8: Granger causal dependency diagrams for encoder 1 and 2 in nominal (left column) and faulty (right column) conditions in curved left motion.

To evaluate the method on a sliding window in this case, the relationship between encoder 1 and encoder 2 is taken into consideration as in the previous section. The change in p-values with the fault in sliding window for curved left motion is shown in Fig.(6.9). It can be seen that p-value is almost consistently minimum when the signals are nominal in both the cases, although there is a small peak with a sudden change in the signal. When the fault is induced by unplugging the encoders, the p-value is inconsistent, and crosses the defined threshold. Thus, it can be concluded that the implemented method works for

the case.



(a) Change in p-value when encoder 1 is unplugged.



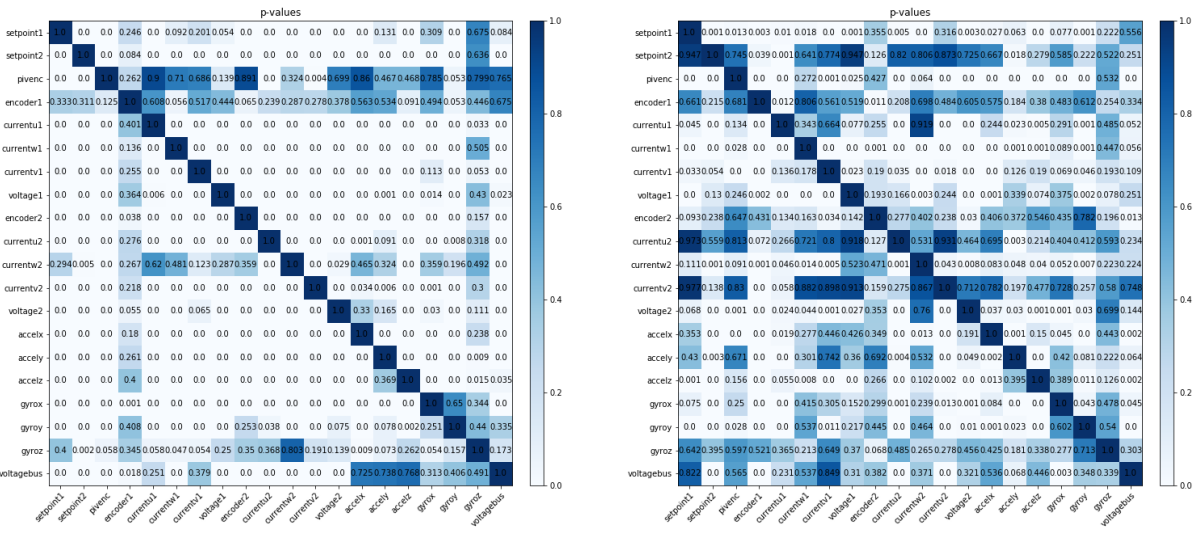
(b) Change in p-value when encoder 2 is unplugged.

Figure 6.9: Change in p-value when fault is introduced by unplugging encoders.

## 6.1. Evaluation in Torque Mode

### Curved Motion Right

The experiments conducted in the previous section is repeated here for the curved motion in the right direction. The p-values from Granger Causality are generated with unplugged encoders are shown in Fig.(6.10). From Fig.(6.10), it can be observed that, the violations with encoder 2 unplugged (shown in Fig.(6.10a)) is more the violations of dependencies caused from unplugging encoder 1 (shown in Fig.(6.10b)).



(a) Curved right motion with encoder1 unplugged.

(b) Curved right motion with encoder2 unplugged.

Figure 6.10: p-values for curved right motion with unplugged encoders.

The dependency diagrams are shown in Fig.(6.11). From the Fig.(6.11), it can be observed that, for nominal conditions, the dependency patterns as shared by encoder 1 and 2 are almost similar. Also, when the encoder 1 is unplugged, the causality from encoder 1 to encoder 2 disappears and vice versa.

Further the dependency detection is tested on a sliding window for the unplugged encoder 1 and encoder 2. The same encoder 1 and encoder 2 signals are considered here, as in the previous sections. Although there are violations of dependencies with other sensor variables, it is easier to visualize change in the signals and violation of dependencies among the encoders as they have same time series pattern resulted from redundancy.

The dependency detection method implemented in this case for the unplugged encoder 1 and encoder 2 are shown in Fig.(6.12). From the Fig.(6.12), it can be observed that the method behaves very well in this case when the signals are nominal, as compared to previous case. There is no peak with the sudden change of signals. However, the response of p-value for the fault is delayed, especially when encoder 1 is unplugged (shown in Fig.(6.12a)). Thus, from the results, it can be concluded that the dependency detection method works for the considered case.

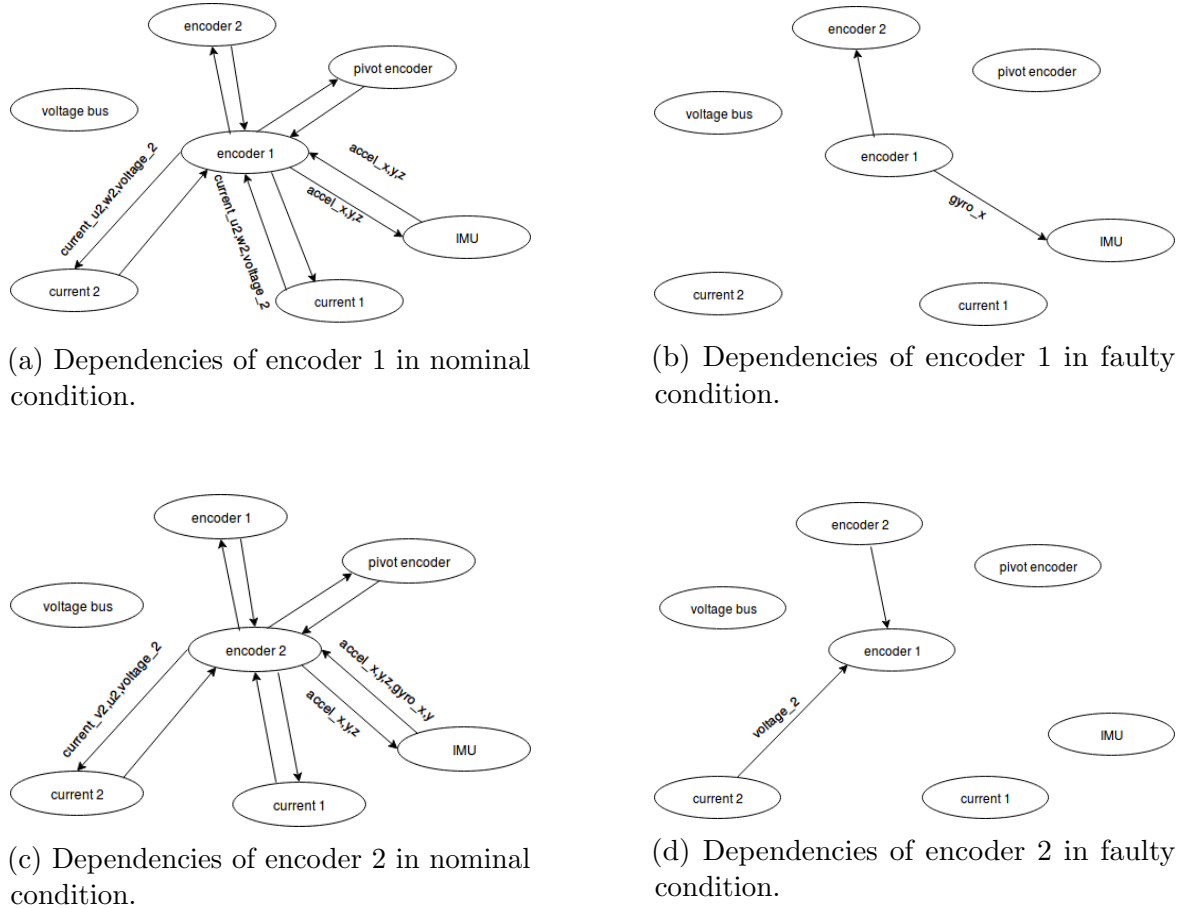
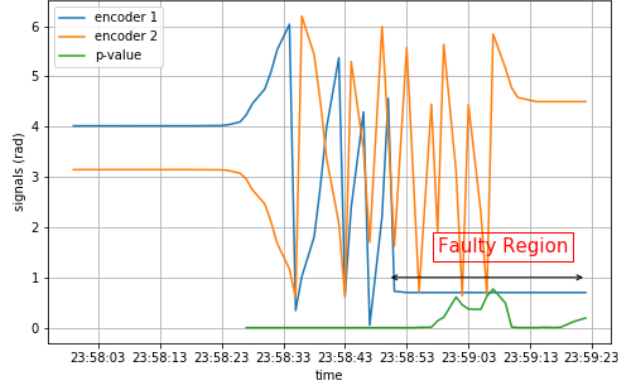
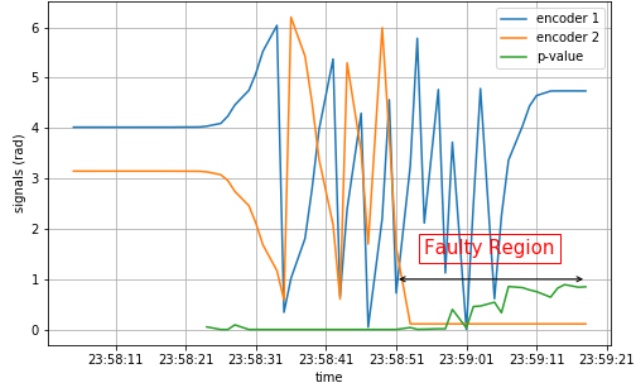


Figure 6.11: Granger causal dependency diagrams for encoder 1 and 2 in nominal (left column) and faulty (right column) conditions in curved right motion.



(a) Change in p-value when encoder 1 is unplugged.



(b) Change in p-value when encoder 2 is unplugged.

Figure 6.12: Change in p-value when fault is introduced by unplugging encoders.

### On Spot Rotation Clockwise

The ropod platform can be rotated 360 degrees on its own axis. In this case, the fault is injected by unplugging encoder 1 of the smart wheel and the platform is rotated in clockwise direction. The p-values generated by unplugging encoder 1 of the smart wheel is shown in Fig.(6.13). It can be observed that almost all the dependencies associated with encoder 1 as in the nominal case, shown in Fig.(6.3a) have disappeared. To get clear idea, the dependencies of encoder 1 in nominal and faulty cases are shown in dependency diagram in Fig(6.14).

From the Fig.(6.14), it can be observed that, with the fault induced, the direction of

## Chapter 6. Experimental Results

---

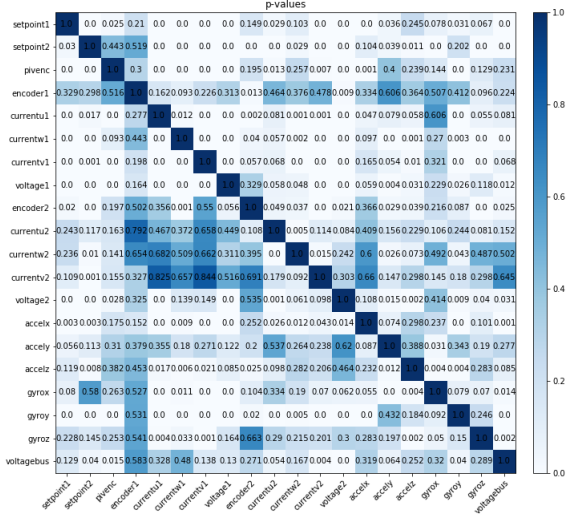


Figure 6.13: p-values for on spot rotation in clockwise direction with unplugged encoder 1.

Granger causality between encoder 1 and encoder 2 are reversed. This may not reveal any true meaning of dependency. It should be noted the p-values are entirely dependent on the prediction capability of one signal on the future values of the other. Thus, a reasonable dependency may not exist in every case. However, this is not a general problem on sliding window of SFDD, as it only checks the continuity of patterns. In other words, if encoder 1 is causing encoder 2 in the history of defined size depending on the size of the window, it is expected to continue the same pattern in the rest of the window. If it doesn't, the fault is expected to be detected.

In the previous sections, encoder 1 and encoder 2 of the considered smart wheel were compared. In this case, the method is demonstrated using other sensed variable the dependency of encoder 1 is violated with. In Fig.(6.14), it is clear that the Granger causality between the encoder 1 value and gyro-y, rotation of the wheel in y axis (measured in rad/s) provided by IMU sensor is violated. The change in p-value with this change in dependency is hence shown on sliding window.

Consider the Fig.(6.15) with signals on encoder 1 and gyro-y on a sliding window with window size 2.5 second. The p-value is almost zero when the signals are nominal, except a small peak at a point. When the encoder gets stuck and the signal becomes flat, there is a sharp increase in p-value.

## 6.1. Evaluation in Torque Mode

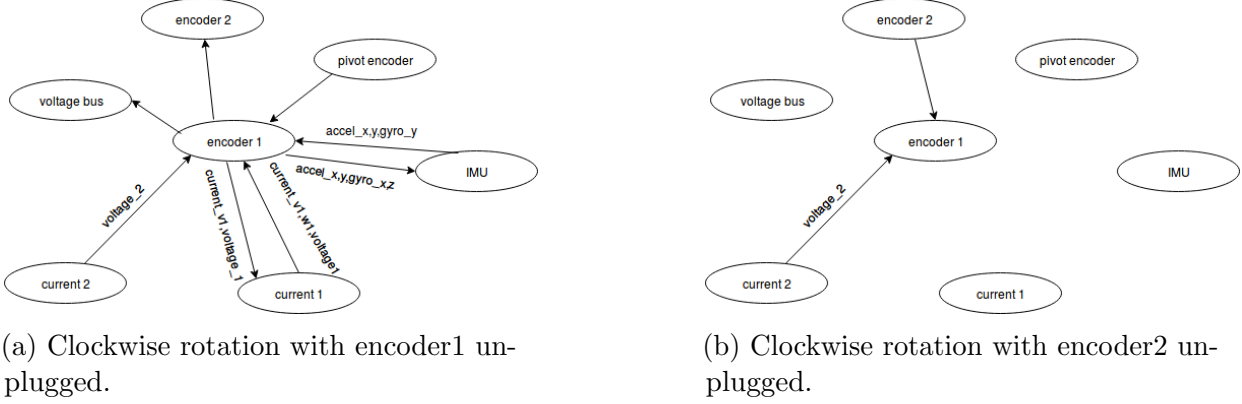


Figure 6.14: Granger causal dependency diagrams for encoder 1 and 2 in nominal (left column) and faulty (right column) conditions in on spot rotation in clockwise direction.

In the middle of the faulty region, the gyro\_y also is close to zero and the signals becomes almost flat. Even in this case, p-value shows a drop indicating a small amount of dependency. Hence, the change in the p-values are reasonable in the considered case. Thus, it can be concluded that the method works fine for this case.

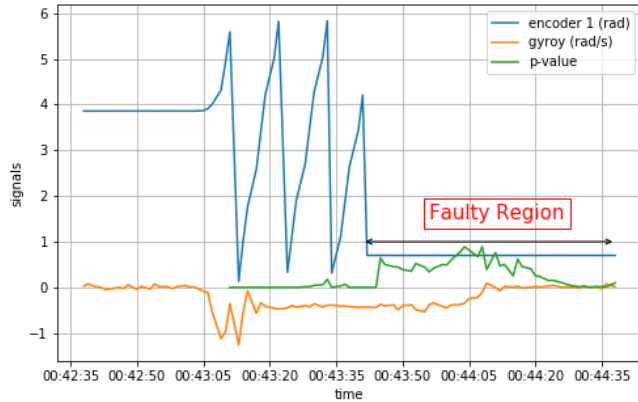


Figure 6.15: Change in p-values for on spot rotation in clockwise direction with unplugged encoder 1.

## Chapter 6. Experimental Results

## On Spot Rotation Anti-clockwise

The experiment from previous section is repeated here for anti-clockwise direction. The encoder 1 sensor from the smart wheel is unplugged and the platform is rotated in anti-clockwise direction. The p-values generated are shown in Fig.(6.16). The violations of dependencies resemble the violations in previous case. It can be observed that, in this case, no dependencies are retained by encoder 1.

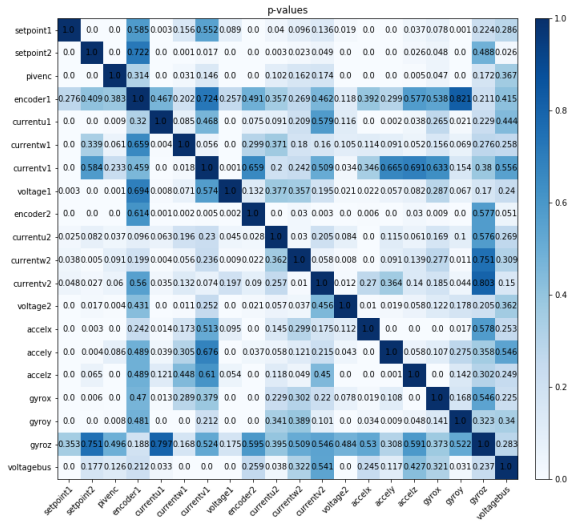


Figure 6.16: p-values for on spot rotation in anti-clockwise direction with unplugged encoder 1.

The dependency diagram for the encoder 1 in nominal and faulty cases are shown in Fig.(6.17). Here, Granger causality exists in both directions between encoder 1 and encoder 2 in the nominal state and the both these dependencies disappear when fault is introduced, unlike the previous case.

Like in clockwise rotation, the dependency between encoder 1 and gyro\_y from IMU sensor is violated in this case, with the occurrence of fault. Hence, the same encoder 1 and gyro\_y are considered here to notice change in p-values with the abrupt change in the signal on sliding window. The signals on sliding window is shown in Fig.(6.18). It can be observed that p-value fluctuates more in this case, as compared to the rotation in clockwise direction. When the signals are in nominal state, there are small peaks in the p-values that are over the threshold. Although the p-values are not as consistent, it can

## 6.1. Evaluation in Torque Mode

be observed that most of the values are close to zero, that enable recognition of non-faulty region in the figure.

However, the p-values have high values when the signals enter faulty region, indicating persistence of faults. Also, it can be observed that, when gyro\_y signal is almost flat in the end of the faulty region, the p-values are still high, unlike in the case of rotation in clockwise direction.

In the cases of straight and curved motions, the signals considered i.e encoder 1 and encoder 2 were correlated, as well as Granger causality existed between the signals. In the case of on spot rotation, the signals considered were not correlated, but Granger causality existed between the signals. This shows that Granger causality does not imply correlation. Also, when the signal gyro\_y was almost flat in the half of the faulty region in clockwise rotation case (shown in Fig.(6.15)), there was some correlation between the signals and the drop of p-value indicated existence of certain Granger causal dependencies. However, when this happened in Fig.(6.18), p-values were high indicating no Granger causality, thus proving correlation does not imply Granger causality either.

This non-existence of Granger causality is more clear in p-values in matrix format with all diagonal elements indicating no Granger causality with high p-value, where the signals are compared with themselves and high correlation is obvious.

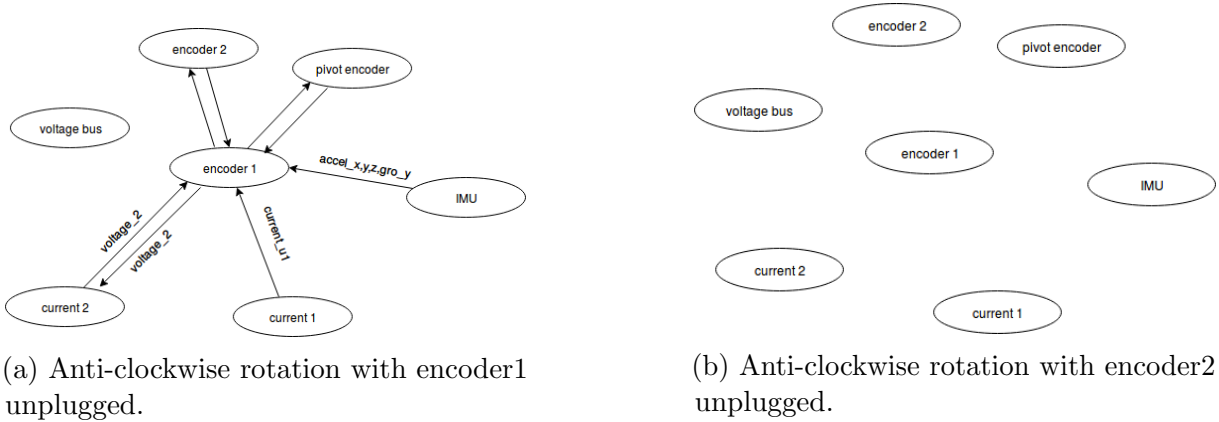


Figure 6.17: Granger causal dependency diagrams for encoder 1 and 2 in nominal (left column) and faulty (right column) conditions in on spot rotation in clockwise direction.

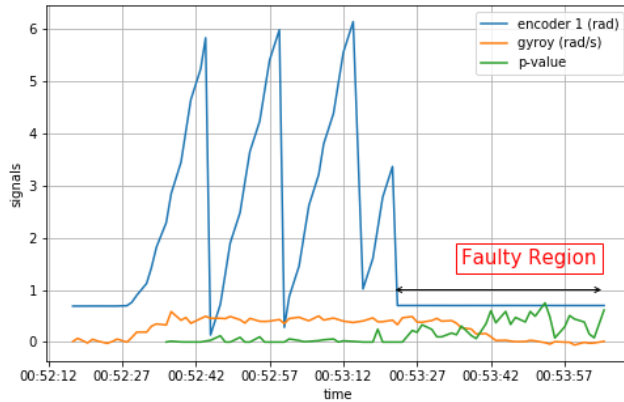


Figure 6.18: Change in p-values for on spot rotation in anti-clockwise direction with unplugged encoder 1.

### 6.1.3 Dependency Detection with Disconnected Power Supply to a Motor

In the previous section the results from the experiment with unplugged wheel encoders in various motions were analyzed. In this section, the results obtained from different previously considered motions, with power supply to one of the motors of the smart wheel are analyzed.

The p-values shown in Fig.(6.19), Fig.(6.20) and Fig.(6.21) show that the current values corresponding to motor 2 (current\_u2,current\_v2,current\_w2,voltage\_2) are high, indicating the fault in power supply to motor 2. But, in on spot rotation, there are violations of plenty of dependencies other than those associated with power supply to motor 2.

As there exists nominal Granger dependency among current\_u1,v1,w1 with current\_u2,v2,w2, and since, there are certainly correlated, enabling clear visualization of change in the signals when faults are introduced, for all the motions, the signals current\_w1 and current\_w2 are shown on sliding window. The change in the p-values when fault is introduced can be easily recognized when the patterns of the signals are same.

## 6.1. Evaluation in Torque Mode

The sliding window for all the motions with the signals current\_w1 and current\_w2 are shown in Fig.(6.22), Fig.(6.23) and Fig.(6.24) for straight motion, curved motions an on spot rotations respectively.

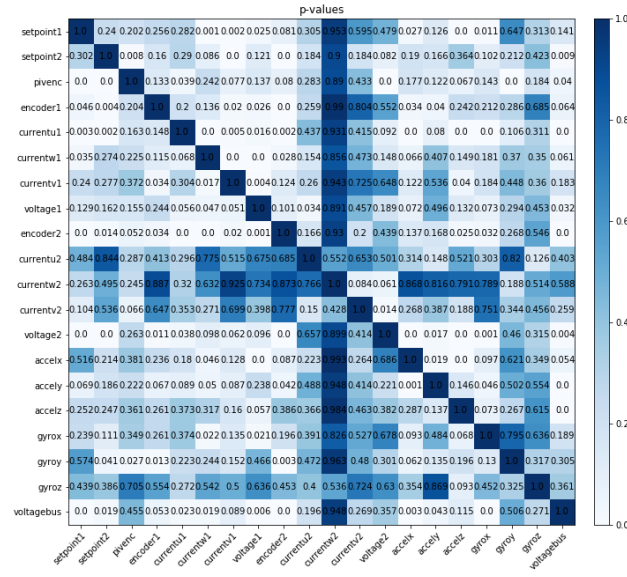


Figure 6.19: p-values for straight motion with disconnected power supply to motor 2.

It can be observed that the current\_w2 value is not stuck as in the case of encoder with the disconnection of power supply. This may possibly the small components between current sensor and output that draw some current that is sensed by the sensor.

The method does not behave well in the case of straight motion shown in Fig.(6.22). The p-values fluctuate continuously and is not consistent. However, the values are higher in the faulty region. The response to the fault also is delayed.

The behavior is same in curved left and curved right motions (shown in Fig.(6.23)). There are small peak values in non-faulty regions. Also, the response to the delay is very high. Fig.(6.24) shows that in on spot rotation, the consistency is high and the change in p-value is fast and sharp. Thus, considering the results from all the motions, it can be concluded that the method behaves moderately in this case.

## Chapter 6. Experimental Results

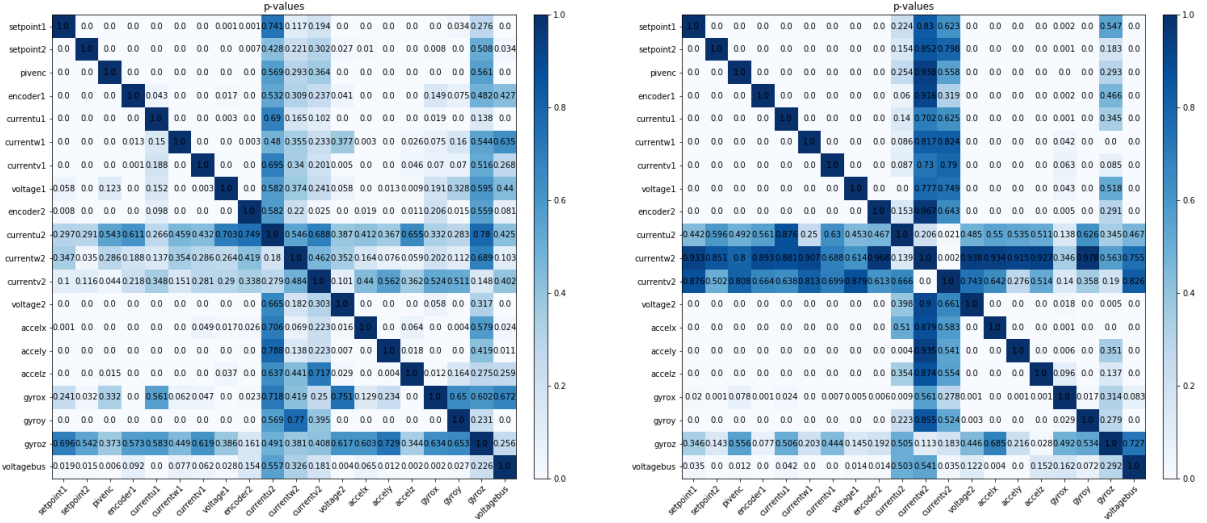


Figure 6.20: p-values for curved motions when power supply to motor 2 is disconnected

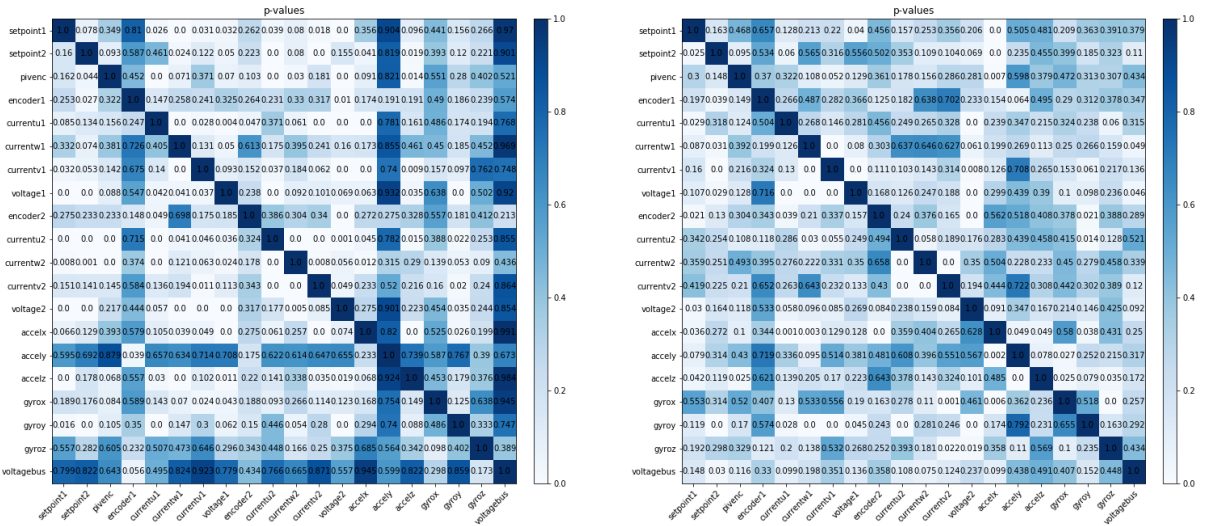


Figure 6.21: p-values for on spot rotations when power supply to motor 2 is disconnected.

## 6.1. Evaluation in Torque Mode

---

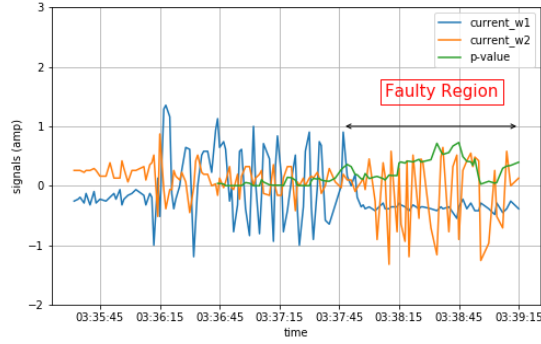
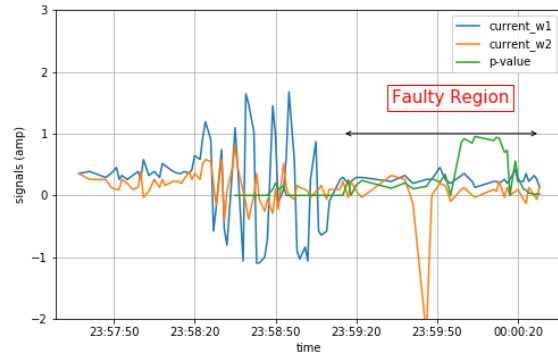
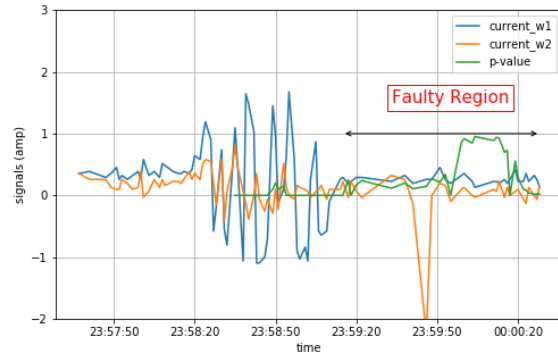


Figure 6.22: Change in p-values with disconnected power supply to motor 2 in straight motion.

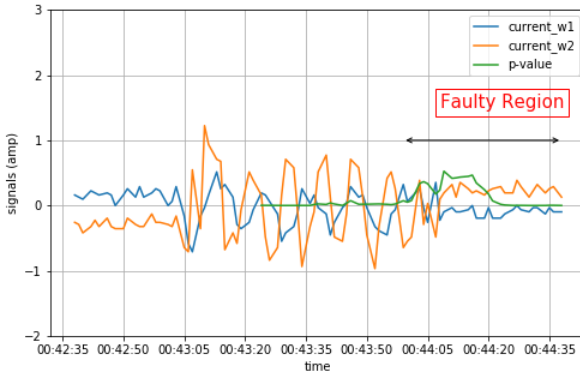


(a) Change in p-values in curved left motion.

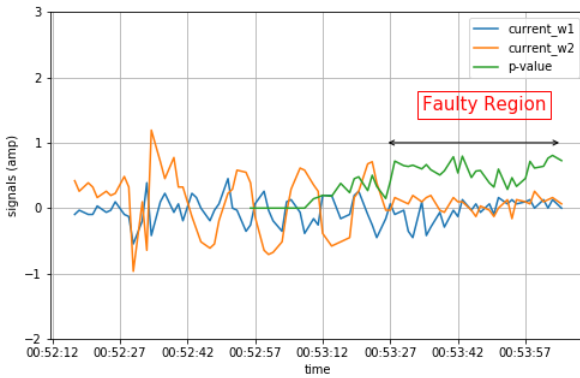


(b) Change in p-values in curved right motion.

Figure 6.23: Change in p-values with disconnected power supply to motor 2 in curved motions.



(a) Change in p-values in clockwise rotation.



(b) Change in p-values in anti-clockwise rotation.

Figure 6.24: Change in p-values with disconnected power supply to motor 2 in on spot rotations.

## 6.2 Evaluation in Velocity Mode

In the previous section the experiments were conducted on the motions generated in torque mode, with the remote controlled velocities. In this section, the results from the experiments in velocity mode are discussed. In velocity mode, the motion of the ropod platform is controlled through program commanded velocities. The variables 'set point1' and 'set point 2' here refer to the commanded velocities (rad/s) for motor 1 and motor 2 of a smart wheel respectively.

In this mode, the experiment is conducted only for straight motion. Further, the faults

are injected by unplugging encoder 1 and encoder 2, one at a time, from the same smart wheel considered in the previous experiments.

### 6.2.1 Defining Nominal Dependencies

Nominal dependency for straight motion in velocity mode is shown in the Fig.(6.25). It can be observed that the dependencies in nominal straight motion in velocity mode, highly resemble the pattern of dependencies in nominal straight motion in torque mode shown in Fig(6.25).

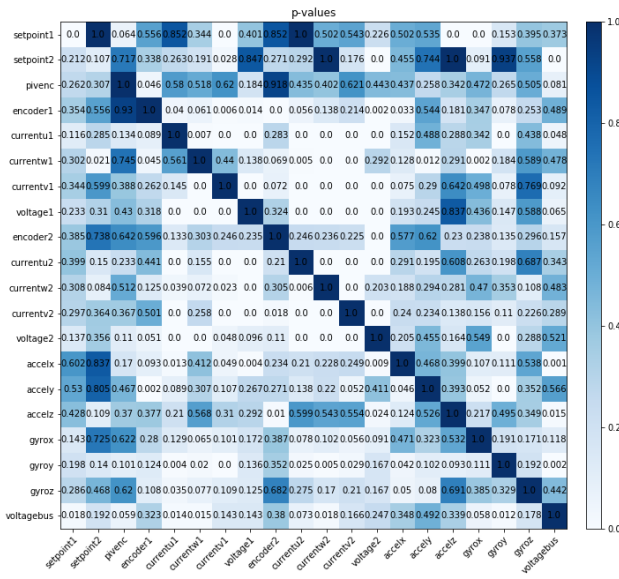


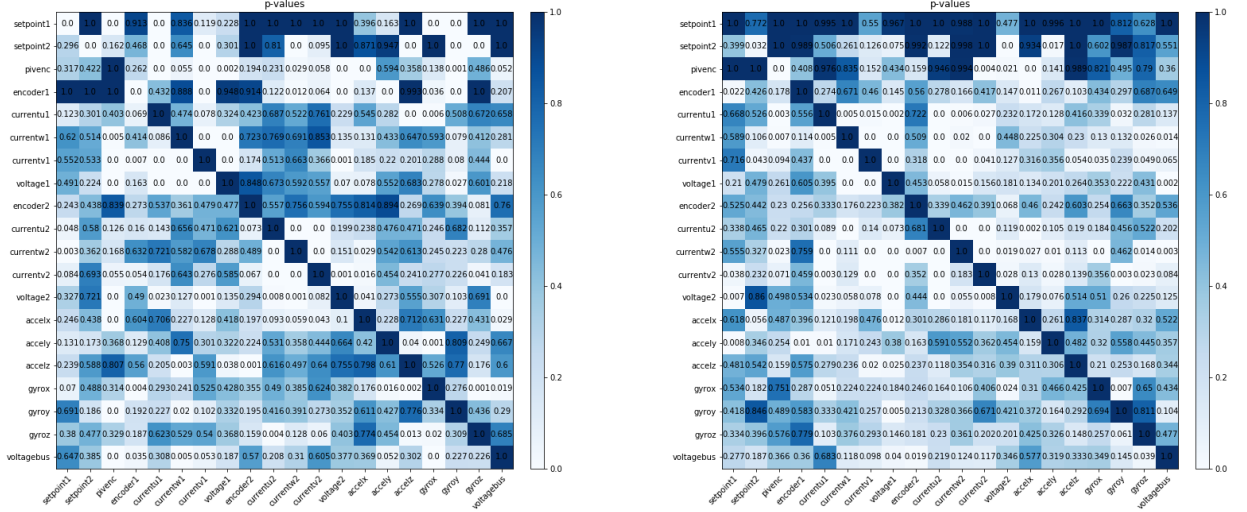
Figure 6.25: Granger causal dependencies defined by p-values for nominal straight motion in velocity mode.

As in the previous section, these dependencies are further used to check the violated dependencies when the fault is injected.

### 6.2.2 Dependency Detection with an Unplugged Wheel Encoder

The same experiment in section 6.1.2 is repeated here for velocity mode. The p-values generated with unplugged encoders are shown in Fig(6.26). In Fig(6.26a), it can be seen that when encoder 1 is unplugged, it Granger causes itself (with p-value 0).

## Chapter 6. Experimental Results



(a) Straight motion with encoder1 unplugged.

(b) Straight motion with encoder2 unplugged.

Figure 6.26: p-values for straight motion with unplugged encoders.

As in the previous sections, the dependency diagrams are shown in Fig.(6.27). For encoder 1, various dependencies are generated when it is unplugged shown in Fig.(6.27b). However, the change in dependency patterns are sufficient to recognize faults. The dependencies existing in nominal cases such as causality from encoder 2 to encoder 1, are violated. Also, the arrow connecting encoder 1 with itself in Fig.(6.27b), indicates existence of Granger causality with itself when it is unplugged.

In the case of encoder 2, almost all the dependencies are violated. Considering the fact that the Granger causality from encoder 2 to encoder 1 is violated in both the cases, the signals for the variables are considered to check the change in p-value with the fault on sliding window.

The sliding window with window size 1.5 second for both the cases are shown in Fig.(6.28). In both the cases, the p-values are very inconsistent. Although, the faulty region is recognizable from the curve of the p-values, with the increase in p-value in faulty region, the threshold is crossed continuously in nominal region, especially when encoder 1 is unplugged, shown in Fig.(6.28a). This may be possibly due to the sudden changes in the signals.

## 6.2. Evaluation in Velocity Mode

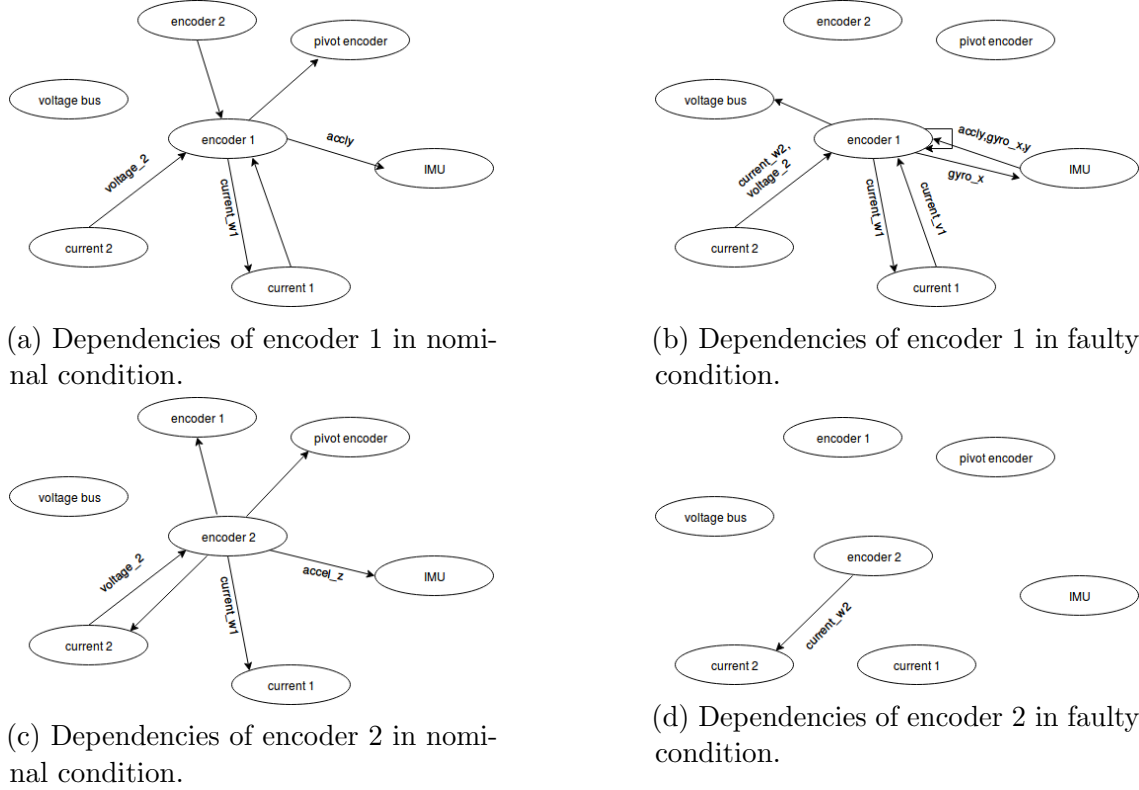
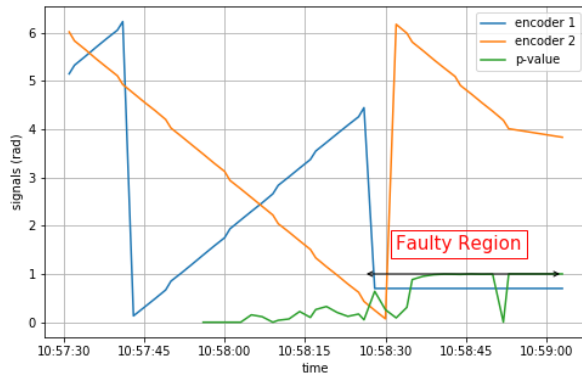
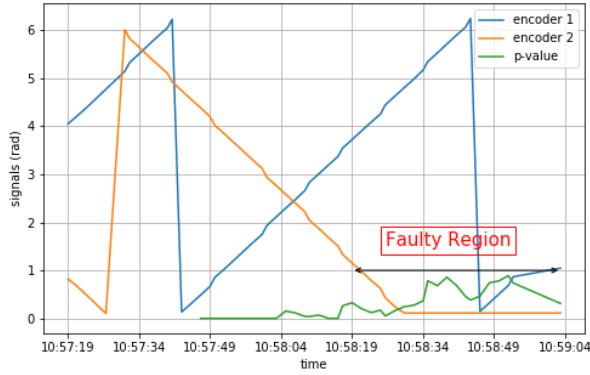


Figure 6.27: Granger causal dependency diagrams for encoder 1 and 2 in nominal (left column) and faulty (right column) conditions in straight motion in velocity mode.



(a) Straight motion with encoder1 unplugged.



(b) Straight motion with encoder2 unplugged.

Figure 6.28: p-values for straight motion with unplugged encoders.

Thus considering the results from both the cases where encoder 1 and 2 are unplugged for straight motion in velocity mode, it can be concluded that the method doesn't behave appreciably in the considered case.

The experimental results show that Granger causality appreciably detects dependencies in most of the cases. In torque mode, Granger causality was clearly able to detect dependencies between encoders. However, it is necessary to note that they do not possess causal relationships. The existence of Granger causality only refers to the ability of one encoder signal to predict the future values of another. Also, in this case, co-existence of Granger causality and correlation is "accidental". These variables were chosen to demonstrate change of p-values on sliding window because it is easy to visualize and interpret faults when dependencies between the signals are more intuitive.

The results from the case with unplugged power supply illustrates the fact that Granger causality does not always work very well with correlated data. While the considered currents were well correlated, the results of Granger causality was moderate. Also, when signals exhibiting clear negative correlation in nominal region of the encoder signals in velocity mode (shown in Fig.(6.28), Granger causality didn't deliver expected results. However, Granger causality exists among less intuitive variables in some cases such as current\_u1 and gyro\_y in Fig.(6.1). These variables with p-value 0 are not an immediate data one would look at to check the performance of a dependency detection method.

On the other hand, correlation also can exist between non-redundant variables. The

## 6.2. Evaluation in Velocity Mode

---

difference is that when sensors are redundant correlation "always" exists. This is not true for Granger causality. No set of variables can be argued to be having Granger causal dependency among them without analysis, which makes the results a little hard to interpret. Also, the existence of Granger causal dependencies are not consistent as p-values vary in each considered case. But, from the results we can see that the method elegantly handles noise and lag and provides acceptable results. Also, the provision of directionality can be exploited in the cases where feedback relationships exist. Hence, considering the merits of Granger causality, it is concluded that it can be successfully applied for sensor dependency detection.

## Conclusions

In this work, state-of-the-art dependency detection methods were reviewed to select a potential sensor dependency detection method that outperforms correlation, for sensor-based fault detection and diagnosis with structural model. A statistical framework, Granger causality was selected for the implementation based on the analysis. The performance of the method was compared against correlation and cross-correlation methods on some sample signals, showing that Granger causality outperforms the methods in various cases, especially in presence of noise and lag in the signals.

Experiments were conducted on the Ropod platform to evaluate the performance of the method in real-time, generating various motion patterns (straight, curve left, curve right motions and on spot rotations in clockwise and anti-clockwise directions). Faults were injected in the system to analyze the behavior of the method in faulty conditions.

The results from the method shows that the dependencies detected by Granger causality are "less intuitive" as compared to correlation. It does not exploit redundant information from the system like any typical dependency detection method and checks the ability of one signal to predict the future values of the other. However, this overcomes a shortcoming of correlation, reliance on redundancy, as mentioned in [27].

The method is robust to noise and lag and outperforms correlation method when data has considerable lag and noise. It also is better than correlation when the complexity in determining the threshold is considered. Threshold determination is crucial in sensor dependency detection, and Correlation and cross-correlation methods are sensitive to threshold value. But, Granger causality practically needs only confidence interval and

dataset as  $p\text{-value} \leq 0.05$  is a universally applied threshold in statistics for Granger causality and it works well for sensor dependency detection.

The method successfully exploits spatial and temporal dependencies and works well on sliding window showing sharp changes when dependencies are violated due to faults in most of the cases. Also, it provides easy computation, which makes it suitable for on-line fault detection and diagnosis. The method is also able to handle diverse set of signals. Most importantly, the properties of Granger causality appears promising to further integrate it with structural model framework. Thus, Granger causality fulfills the objectives of the problem statement and from the analysis of characteristics of Granger causality and results of the experiments in this work, it can be concluded that Granger causality is suitable for sensor-dependency detection.

## 7.1 Contributions

The major contributions of this work are listed as follows:

- A review of state-of-the-art methods for sensor dependency detection.
- Implementation of an alternate method for sensor dependency detection.
- Comparison of the method against existing potential methods (correlation and cross-correlation) on sample simulated data.
- Evaluation of the performance of the method on a real-time scenario.

## 7.2 Lessons learned

The work helped in realizing the criticality and importance of fault detection and diagnosis methods, specifically in autonomous systems. Exploring more on fault diagnosis approaches gave a better understanding of several system control related concepts and helped in gaining more insights on fault propagation, identification and isolation.

## 7.3 Future work

The Granger causality method applied here uses bivariate VAR model that exploits the relationships between only couple of data streams. This can be extended to exploit

## Chapter 7. Conclusions

---

relationships among multiple data streams by replacing bivariate VAR model with multi-variate VAR model. An alternate method can be implemented to find the best p-value, such as Akaike Information Criterion (AIC) or Schwarz Information Criterion to get more dependable results.

The work only demonstrates sensor-dependency detection. This can be integrated with sensor-based fault detection and diagnosis (SFDD) method to analyze the overall impact of the method in real-time fault detection. This can be further compared with SFDD method with correlation to draw concrete conclusions.



A

## Nominal Signals from Ropod Platform

The plots of the signals of sensor variables obtained from a smart wheel of the ropod platform from various motions are given here. The units of the signals can be referred from table 5.1.

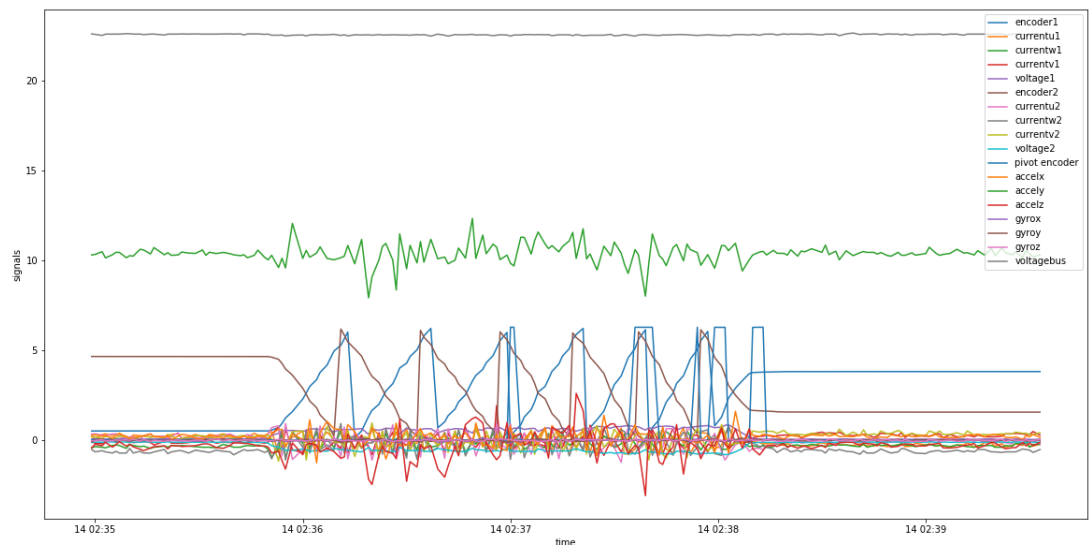


Figure A.1: Nominal sensed signals from straight motion in torque mode.

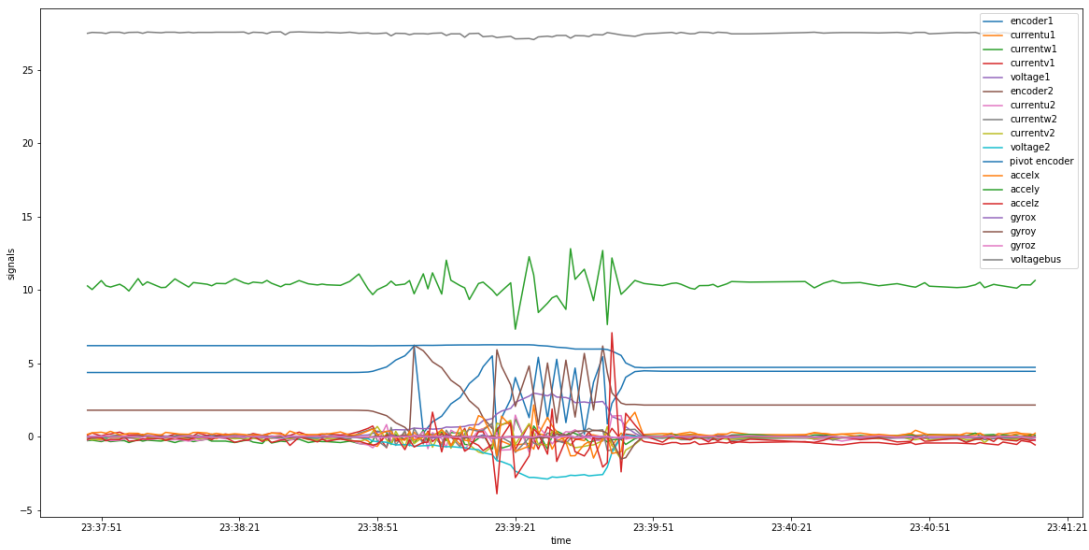


Figure A.2: Nominal sensed signals from curved left motion in torque mode.

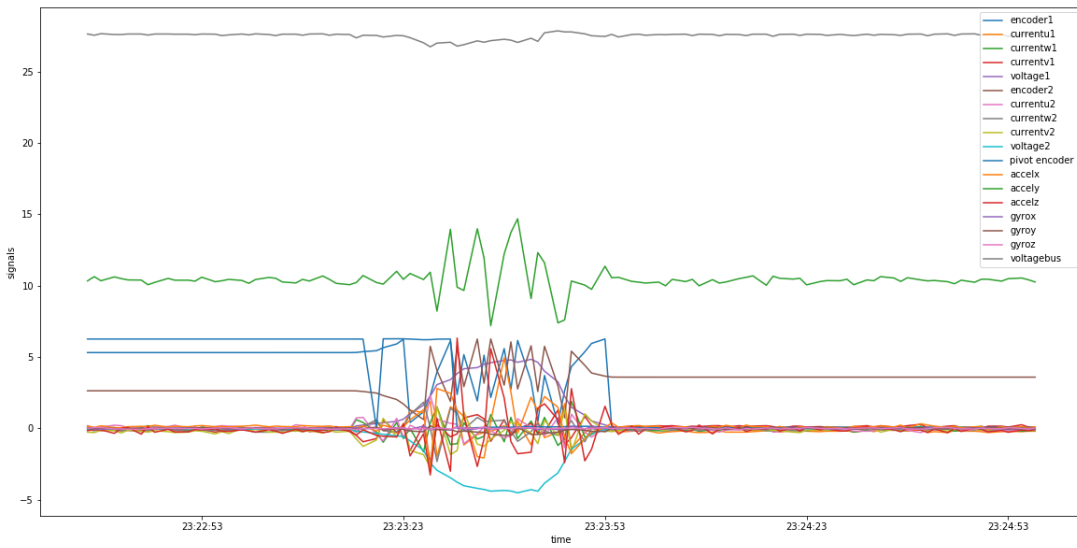


Figure A.3: Nominal sensed signals from curved right in torque mode.

## Appendix A. Nominal Signals from Ropod Platform

---

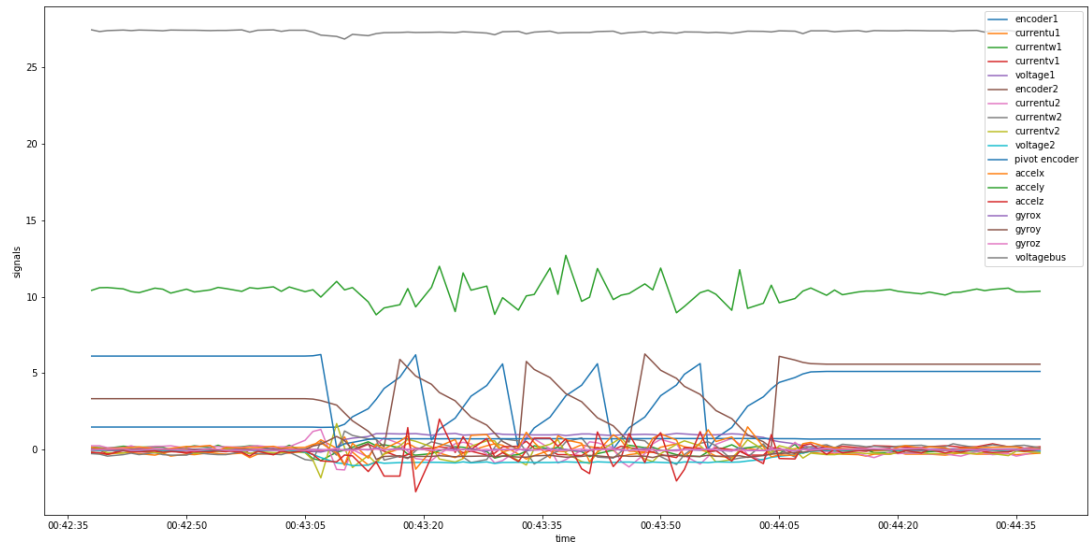


Figure A.4: Nominal sensed signals from on spot rotation in clockwise direction in torque mode.

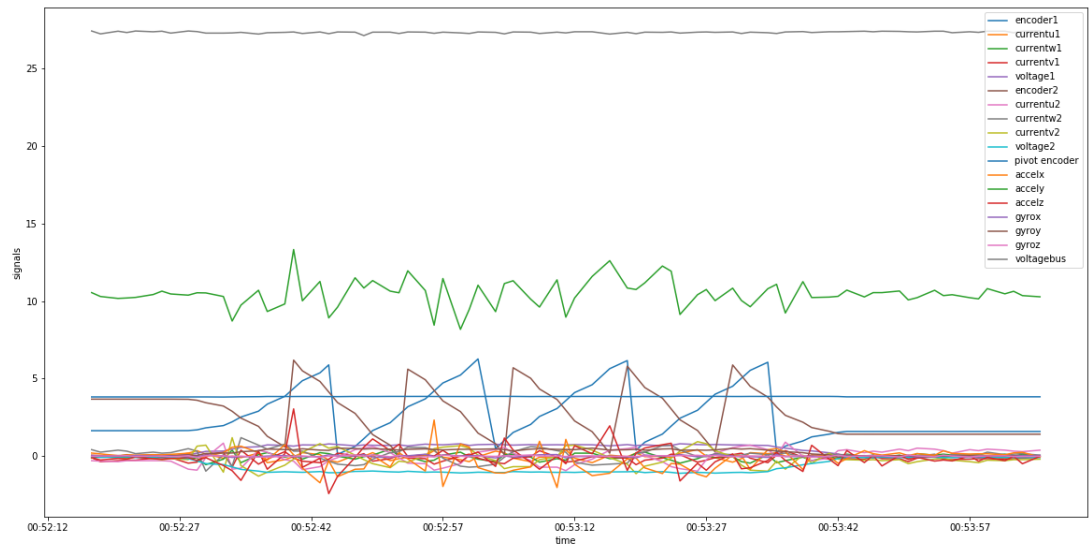


Figure A.5: Nominal sensed signals from on spot rotation in anti-clockwise direction in torque mode.

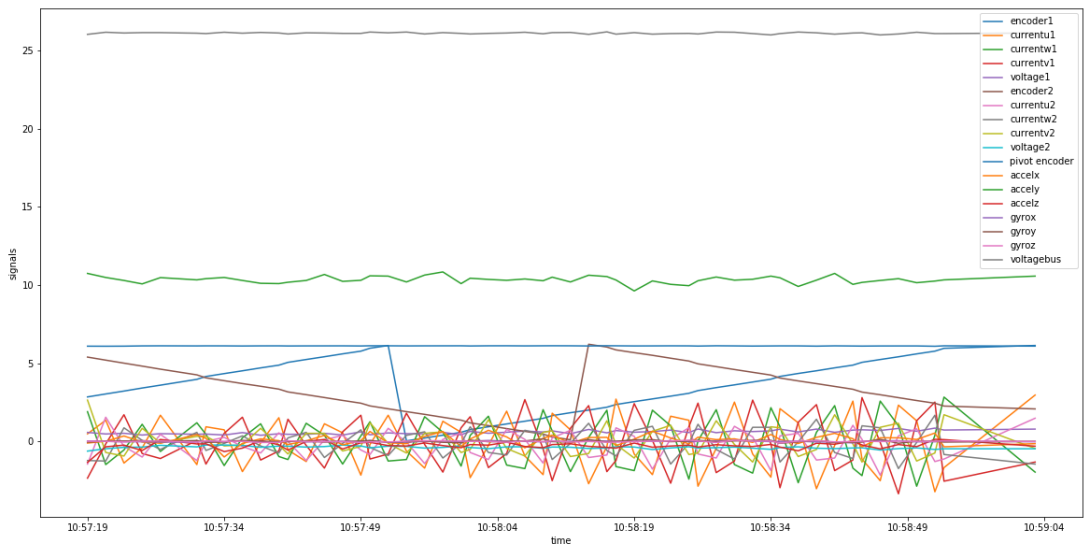


Figure A.6: Nominal sensed signals from straight motion in velocity mode.

## References

- [1] Stationarity and differencing. URL <https://people.duke.edu/~rnau/411diff.htm>. [Online; accessed 13-January-2019].
- [2] Walter A. Shewhart. Economic control of quality of manufactured product. *Bell System Technical Journal*, 9, 04 1930. doi: 10.1002/j.1538-7305.1930.tb00373.x.
- [3] M. Abdelrahman, P. Kandasamy, and J. Frolik. A methodology for the fusion of redundant sensors. In *Proceedings of the 2000 American Control Conference. ACC (IEEE Cat. No.00CH36334)*, volume 4, pages 2922–2926 vol.4, June 2000. doi: 10.1109/ACC.2000.878745.
- [4] C. Alippi, S. Ntalampiras, and M. Roveri. A cognitive fault diagnosis system for distributed sensor networks. *IEEE Transactions on Neural Networks and Learning Systems*, 24(8):1213–1226, Aug 2013. ISSN 2162-237X. doi: 10.1109/TNNLS.2013.2253491.
- [5] C. Alippi, M. Roveri, and F. Trov. Learning causal dependencies to detect and diagnose faults in sensor networks. In *2014 IEEE Symposium on Intelligent Embedded Systems (IES)*, pages 34–41, Dec 2014. doi: 10.1109/INTELES.2014.7008983.
- [6] Saugata Biswas. Deployment of a correlation based algorithm for a robotic black box. Master’s thesis, Bonn-Rhein-Sieg University of Applied Sciences, Grantham-Allee 20, 53757 St. Augustin, Germany, September 2017.
- [7] Yuval Bitan and Michael F OConnor. Correlating data from different sensors to increase the positive predictive value of alarms: an empiric assessment. *F1000Research*, 11 2012. doi: 10.3410/f1000research.1-45.v1.

- [8] Andrew Chernih, Mateusz Maj, Steven Vanduffel, and K U Leuven. Beyond correlations: The use and abuse of copulas in economic capital calculations. *Belgian Actuarial Bulletin*, 04 2007.
- [9] Robert T. Clemen and Terence Reilly. Correlations and copulas for decision and risk analysis. *Management Science*, 45(2):208–224, 1999. doi: 10.1287/mnsc.45.2.208. URL <https://doi.org/10.1287/mnsc.45.2.208>.
- [10] Roger T. Dean and William T. M. Dunsmuir. Dangers and uses of cross-correlation in analyzing time series in perception, performance, movement, and neuroscience: The importance of constructing transfer function autoregressive models. *Behavior Research Methods*, 48(2):783–802, Jun 2016. ISSN 1554-3528. doi: 10.3758/s13428-015-0611-2. URL <https://doi.org/10.3758/s13428-015-0611-2>.
- [11] Ricardo Dunia, S. Joe Qin, Thomas F. Edgar, and Thomas J. McAvoy. Identification of faulty sensors using principal component analysis. *AICHE Journal*, 42(10):2797–2812. doi: 10.1002/aic.690421011. URL <https://onlinelibrary.wiley.com/doi/abs/10.1002/aic.690421011>.
- [12] Eric Torkia. Copulas vs. correlation, 2011. URL <https://www.crystalballservices.com/Research/Articles-on-Analytics-Risk/Post/936/Copulas-Vs-Correlation>. [Online; accessed 13-January-2019].
- [13] Pasquale Foresti. Testing for granger causality between stock prices and economic growth. Mpra paper, University Library of Munich, Germany, 2007. URL [https://mpra.ub.uni-muenchen.de/2962/1/MPRA\\_paper\\_2962.pdf](https://mpra.ub.uni-muenchen.de/2962/1/MPRA_paper_2962.pdf).
- [14] P.M. Frank. Analytical and qualitative model-based fault diagnosis a survey and some new results. *European Journal of Control*, 2(1):6 – 28, 1996. ISSN 0947-3580. doi: [https://doi.org/10.1016/S0947-3580\(96\)70024-9](https://doi.org/10.1016/S0947-3580(96)70024-9). URL <http://www.sciencedirect.com/science/article/pii/S0947358096700249>.
- [15] J. Frolik, M. Abdelrahman, and P. Kandasamy. A confidence-based approach to the self-validation, fusion and reconstruction of quasi-redundant sensor data. *IEEE Transactions on Instrumentation and Measurement*, 50(6):1761–1769, Dec 2001. ISSN 0018-9456. doi: 10.1109/19.982977.

## References

---

- [16] K. Goebel and W. Yan. Correcting sensor drift and intermittency faults with data fusion and automated learning. *IEEE Systems Journal*, 2(2):189–197, June 2008. ISSN 1932-8184. doi: 10.1109/JSYST.2008.925262.
- [17] Clive Granger. Investigating causal relations by econometric models and cross-spectral methods. *Econometrica*, 37(3):424–38, 1969. URL <https://EconPapers.repec.org/RePEc:ecm:emetrp:v:37:y:1969:i:3:p:424-38>.
- [18] Yasmine Harbi, Zibouda Aliouat, and Sarra Hammoudi. Enhancement of iot applications dependability using bayesian networks. In Abdelmalek Amine, Malek Mouhoub, Otmane Ait Mohamed, and Bachir Djebbar, editors, *Computational Intelligence and Its Applications*, pages 487–497, Cham, 2018. Springer International Publishing. ISBN 978-3-319-89743-1.
- [19] Harold Gutch. Correlations and granger causality, 2009. URL <http://www.nld.ds.mpg.de/~timeseries/presentations/harold.pdf>. [Online; accessed 13-January-2019].
- [20] M. Hashimoto, H. Kawashima, T. Nakagami, and F. Oba. Sensor fault detection and identification in dead-reckoning system of mobile robot: interacting multiple model approach. In *Proceedings 2001 IEEE/RSJ International Conference on Intelligent Robots and Systems. Expanding the Societal Role of Robotics in the the Next Millennium (Cat. No.01CH37180)*, volume 3, pages 1321–1326 vol.3, Oct 2001. doi: 10.1109/IROS.2001.977165.
- [21] M. Hashimoto, H. Kawashima, and F. Oba. A multi-model based fault detection and diagnosis of internal sensors for mobile robot. In *Proceedings 2003 IEEE/RSJ International Conference on Intelligent Robots and Systems (IROS 2003) (Cat. No.03CH37453)*, volume 4, pages 3787–3792 vol.3, Oct 2003. doi: 10.1109/IROS.2003.1249744.
- [22] S. Jadhav and R. Daruwala. 3-d modeling of statistical dependencies using copulas for wireless sensor network. In *2016 International Conference on Wireless Communications, Signal Processing and Networking (WiSPNET)*, pages 1886–1889, March 2016. doi: 10.1109/WiSPNET.2016.7566469.

- [23] Ankur Jain, Edward Y. Chang, and Yuan-Fang Wang. Bayesian reasoning for sensor group-queries and diagnosis. In Ramamohanarao Kotagiri, P. Radha Krishna, Mukesh Mohania, and Ekawit Nantajeewarawat, editors, *Advances in Databases: Concepts, Systems and Applications*, pages 522–538, Berlin, Heidelberg, 2007. Springer Berlin Heidelberg. ISBN 978-3-540-71703-4.
- [24] Jeffrey Russel. Vector autoregressive model. URL <http://faculty.chicagobooth.edu/jeffrey.russell/teaching/timeseries/handouts/notes5.pdf>. [Online; accessed 31-December-2018].
- [25] Gatan Kerschen, Pascal De Boe, J.-C Golinval, and Keith Worden. Sensor validation using principal component analysis. *Smart Mater. Struct.*, 14:36–42, 02 2005. doi: 10.1088/0964-1726/14/1/004.
- [26] Eliahu Khalastchi, Gal A. Kaminka, Meir Kalech, and Raz Lin. Online anomaly detection in unmanned vehicles. In *AAMAS*, 2011.
- [27] Eliahu Khalastchi, Meir Kalech, and Lior Rokach. Sensor fault detection and diagnosis for autonomous systems, 01 2013.
- [28] Eliahu Khalastchi, Meir Kalech, and Lior Rokach. A hybrid approach for fault detection in autonomous physical agents. In *AAMAS*, 2014.
- [29] Lutz Kilian and Helmut Ltkepohl. *Structural Vector Autoregressive Analysis*. Themes in Modern Econometrics. Cambridge University Press, 2017. doi: 10.1017/9781108164818.
- [30] Jure Leskovec. Analytics on time series data, 2017. URL [http://www.uh.edu/~bsorense/gra\\_caus.pdf](http://www.uh.edu/~bsorense/gra_caus.pdf). [Online; accessed 29-December-2018].
- [31] R. Lin, E. Khalastchi, and G. A. Kaminka. Detecting anomalies in unmanned vehicles using the mahalanobis distance. In *2010 IEEE International Conference on Robotics and Automation*, pages 3038–3044, May 2010. doi: 10.1109/ROBOT.2010.5509781.
- [32] H. Liu, M. Huang, I. Janghorban, P. Ghorbannezhad, and C. Yoo. Faulty sensor detection, identification and reconstruction of indoor air quality measurements in a subway station. In *2011 11th International Conference on Control, Automation and Systems*, pages 323–328, Oct 2011.

## References

---

- [33] Q. Liu, Y. Yang, and X. Qiu. A metric-correlation-based distributed fault detection approach in wireless sensor networks. In *2015 17th Asia-Pacific Network Operations and Management Symposium (APNOMS)*, pages 186–191, Aug 2015. doi: 10.1109/APNOMS.2015.7275424.
- [34] A. Mahapatro and P. M. Khilar. Fault diagnosis in wireless sensor networks: A survey. *IEEE Communications Surveys Tutorials*, 15(4):2000–2026, Fourth 2013. ISSN 1553-877X. doi: 10.1109/SURV.2013.030713.00062.
- [35] Claudio Giovanni Mattera, Joseba Quevedo, Teresa Escobet, Hamid Reza Shaker, and Muhyiddine Jradi. A method for fault detection and diagnostics in ventilation units using virtual sensors. *Sensors*, 18(11), 2018. ISSN 1424-8220. doi: 10.3390/s18113931. URL <http://www.mdpi.com/1424-8220/18/11/3931>.
- [36] Juan Pablo Mendoza. Mobile robot fault detection based on redundant information statistics. 2012.
- [37] Michael Hauser. Vector autoregressions. URL [http://statmath.wu.ac.at/~hauser/LVs/FinEtricsQF/FEtrics\\_Chp2.pdf](http://statmath.wu.ac.at/~hauser/LVs/FinEtricsQF/FEtrics_Chp2.pdf). [Online; accessed 01-January-2019].
- [38] Michael Murray. A drunk and her dog: An illustration of cointegration and error correction. *American Statistician - AMER STATIST*, 48:37–39, 02 1994. doi: 10.1080/00031305.1994.10476017.
- [39] Wonbin Na, Changwoo Park, Seokjoo Lee, Seongo Yu, and Hyeongcheol Lee. Sensitivity-based fault detection and isolation algorithm for road vehicle chassis sensors. *Sensors*, 18(8), 2018. ISSN 1424-8220. doi: 10.3390/s18082720. URL <http://www.mdpi.com/1424-8220/18/8/2720>.
- [40] Richard E. Neapolitan. *Learning Bayesian Networks*. Prentice-Hall, Inc., Upper Saddle River, NJ, USA, 2003. ISBN 0130125342.
- [41] Roger B. Nelsen. Properties and applications of copulas: A brief survey, 2002.
- [42] Quantstart Team. Autoregressive integrated moving average arima(p, d, q) models for time series analysis, 2012. URL <https://www.quantstart.com/articles/Autoregressive-Integrated-Moving-Average-ARIMA-p-d-q-Models-for-Time-Series-An> [Online; accessed 30-December-2018].

- [43] Quantstart Team. White noise and random walks in time series analysis, 2012. URL <https://www.quantstart.com/articles/White-Noise-and-Random-Walks-in-Time-Series-Analysis>. [Online; accessed 31-December-2018].
- [44] S. I. Roumeliotis, G. S. Sukhatme, and G. A. Bekey. Fault detection and identification in a mobile robot using multiple-model estimation. In *Proceedings. 1998 IEEE International Conference on Robotics and Automation (Cat. No.98CH36146)*, volume 3, pages 2223–2228 vol.3, May 1998. doi: 10.1109/ROBOT.1998.680654.
- [45] S. I. Roumeliotis, G. S. Sukhatme, and G. A. Bekey. Sensor fault detection and identification in a mobile robot. In *Proceedings. 1998 IEEE/RSJ International Conference on Intelligent Robots and Systems. Innovations in Theory, Practice and Applications (Cat. No.98CH36190)*, volume 3, pages 1383–1388 vol.3, Oct 1998. doi: 10.1109/IROS.1998.724781.
- [46] SCCN. Cross-correlation does not imply granger causation, 2012. URL [https://sccn.ucsd.edu/wiki/Chapter\\_4.5.\\_\(Cross-\)\\_correlation\\_does\\_not\\_imply\\_\(Granger-\)\\_causation](https://sccn.ucsd.edu/wiki/Chapter_4.5._(Cross-)_correlation_does_not_imply_(Granger-)_causation). [Online; accessed 30-December-2018].
- [47] Anil K. Seth, Adam B. Barrett, and Lionel Barnett. Granger causality analysis in neuroscience and neuroimaging. *Journal of Neuroscience*, 35(8):3293–3297, 2015. ISSN 0270-6474. doi: 10.1523/JNEUROSCI.4399-14.2015. URL <http://www.jneurosci.org/content/35/8/3293>.
- [48] StatsModels. Statistical tools for time series analysis. URL <http://www.statsmodels.org/dev/generated/statsmodels.tsa.stattools.grangercausalitytests>. [Online; accessed 01-January-2019].
- [49] A. Subramanian, A. Sundaresan, and P. K. Varshney. Fusion for the detection of dependent signals using multivariate copulas. In *14th International Conference on Information Fusion*, pages 1–8, July 2011.
- [50] Analytics University. What is granger causality? URL <https://www.youtube.com/watch?v=ZUv7T8iPGrc>. [Online; accessed 27-December-2018].

## References

---

- [51] Venkat Venkatasubramanian, Raghunathan Rengaswamy, Kewen Yin, and Surya N. Kavuri. A review of process fault detection and diagnosis: Part i: Quantitative model-based methods. *Computers & Chemical Engineering*, 27(3):293 – 311, 2003. ISSN 0098-1354. doi: [https://doi.org/10.1016/S0098-1354\(02\)00160-6](https://doi.org/10.1016/S0098-1354(02)00160-6). URL <http://www.sciencedirect.com/science/article/pii/S0098135402001606>.
- [52] Wikipedia contributors. Granger causality — Wikipedia, the free encyclopedia, 2018. URL [https://en.wikipedia.org/w/index.php?title=Granger\\_causality&oldid=874892208](https://en.wikipedia.org/w/index.php?title=Granger_causality&oldid=874892208). [Online; accessed 27-December-2018].
- [53] Wikipedia contributors. Causality — Wikipedia, the free encyclopedia, 2018. URL <https://en.wikipedia.org/w/index.php?title=Causality&oldid=875810126>. [Online; accessed 29-December-2018].
- [54] Wikipedia contributors. Time series — Wikipedia, the free encyclopedia, 2018. URL [https://en.wikipedia.org/w/index.php?title=Time\\_series&oldid=874419681](https://en.wikipedia.org/w/index.php?title=Time_series&oldid=874419681). [Online; accessed 29-December-2018].
- [55] Wikipedia contributors. Vector autoregression — Wikipedia, the free encyclopedia, 2018. URL [https://en.wikipedia.org/w/index.php?title=Vector\\_autoregression&oldid=872953211](https://en.wikipedia.org/w/index.php?title=Vector_autoregression&oldid=872953211). [Online; accessed 30-December-2018].
- [56] H. Zhang, J. Liu, and R. Li. Fault detection for medical body sensor networks under bayesian network model. In *2015 11th International Conference on Mobile Ad-hoc and Sensor Networks (MSN)*, pages 37–42, Dec 2015. doi: 10.1109/MSN.2015.21.